

SEISMOLOGY

Master Degree Programme in Physics - UNITS
Physics of the Earth and of the Environment

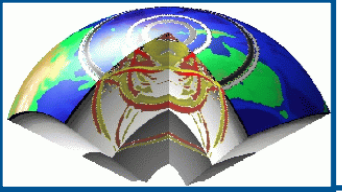
SEISMIC SOURCES 3: FOCAL MECHANISMS

FABIO ROMANELLI

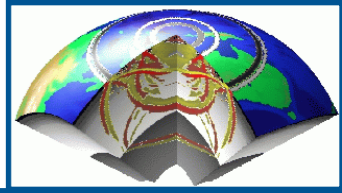
Department of Mathematics & Geosciences

University of Trieste

romanel@units.it



Seismic sources - 3

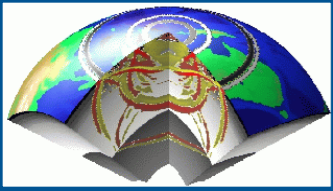


Focal mechanisms

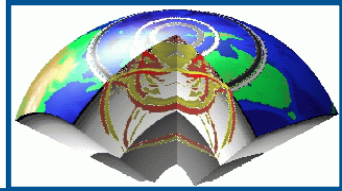
- faulting and radiation pattern
- fault mechanism
- decomposition of moment tensor
- basic fault plane solutions
- faults and plates

Haskell model

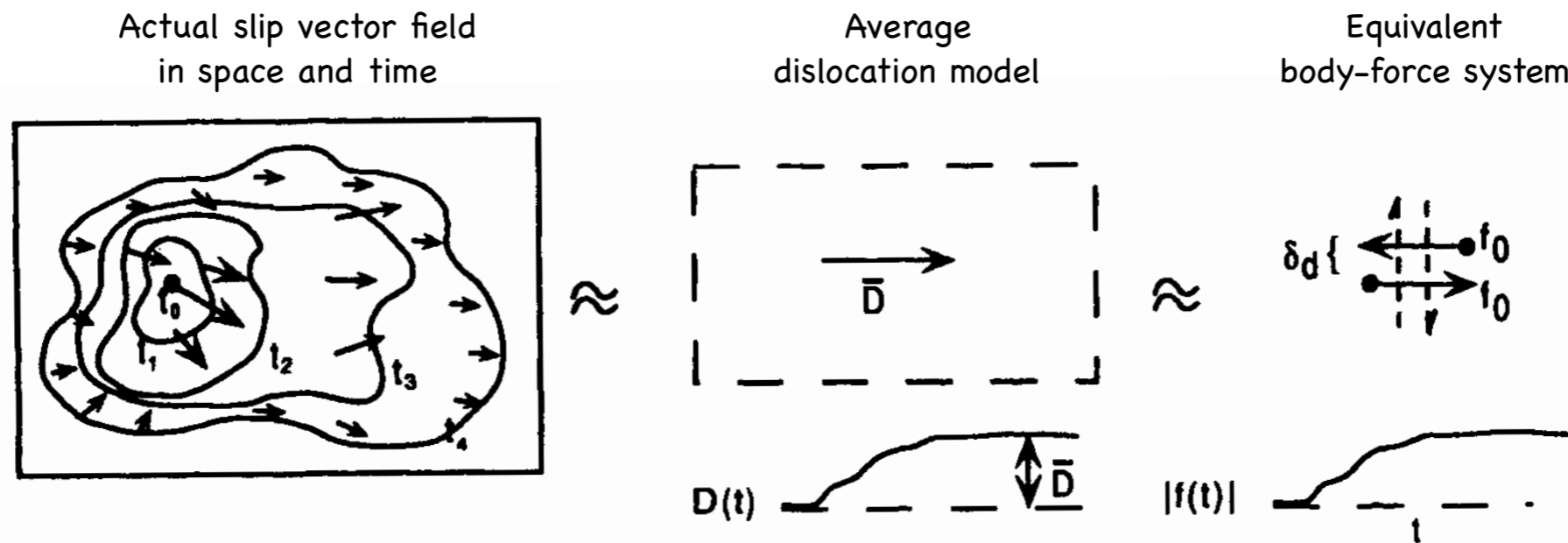
- far field for an extended source
- directivity
- source spectra



Equivalent Forces: concepts

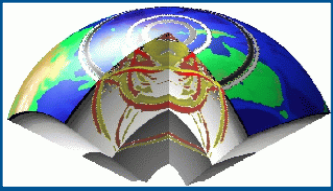


The observable seismic radiation is through energy release as the fault surface moves: formation and propagation of a crack. This complex dynamical problem can be studied by kinematical equivalent approaches.

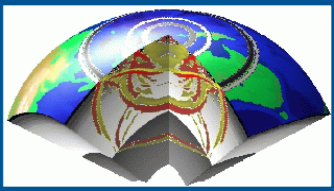


The scope is to develop a representation of the displacement generated in an elastic body in terms of the quantities that originated it: body forces and applied tractions and displacements over the surface of the body.

The actual slip process will be described by superposition of equivalent body forces acting in space (over a fault) and time (rise time).



Moment tensor

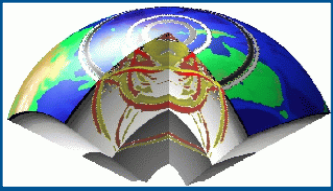


For an isotropic solid, and for **slip parallel** to Σ at ξ , one has respectively:

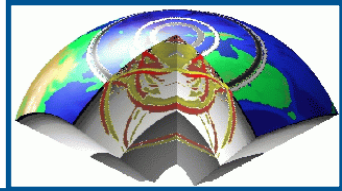
$$m_{pq} = \lambda v_k [u_k] \delta_{pq} + \mu \left(v_p [u_q] + v_q [u_p] \right) \quad m_{pq} = \mu \left(v_p [u_q] + v_q [u_p] \right)$$

And if the source can be considered a point-source (for wavelengths greater than fault dimensions), the contributions from different surface elements can be considered in phase. Thus for an effective **point source**, one can define the **moment tensor**:

$$M_{pq} = \iint_{\Sigma} m_{pq} d\Sigma$$
$$u_n(\mathbf{x}, t) = M_{pq} * G_{np,q}$$



A particular case - moment tensor

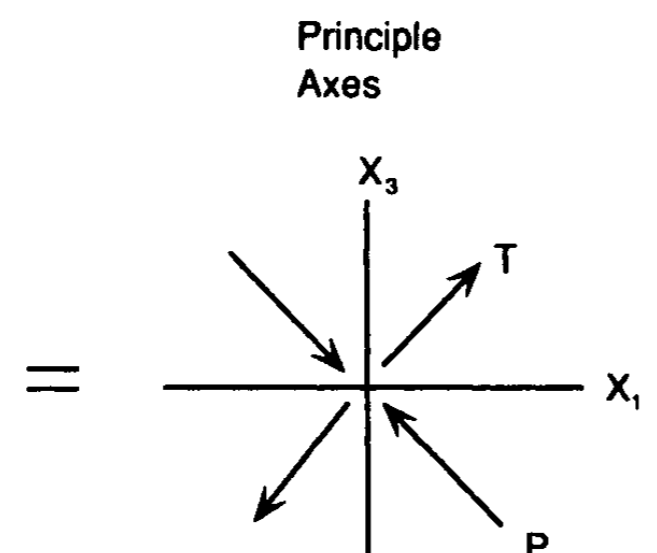
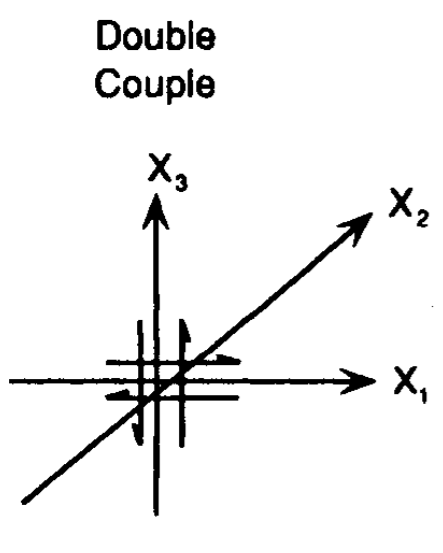


$$\mathbf{m} = \begin{pmatrix} 0 & 0 & \mu[u_1(\xi, \tau)] \\ 0 & 0 & 0 \\ \mu[u_1(\xi, \tau)] & 0 & 0 \end{pmatrix} \quad \mathbf{M} = \begin{pmatrix} 0 & 0 & M_0 \\ 0 & 0 & 0 \\ M_0 & 0 & 0 \end{pmatrix}$$

$\phi=0^\circ, \delta=0^\circ, \lambda=0^\circ$

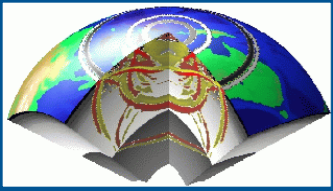
$$\mathbf{u} = \begin{cases} [\bar{u}]\hat{\mathbf{e}}_x \\ 0 \\ 0 \end{cases} \quad \mathbf{v} = \begin{cases} 0 \\ 0 \\ \hat{\mathbf{e}}_z \end{cases}$$

$$\left. \begin{aligned} \mathbf{t} &= \frac{1}{\sqrt{2}} (\hat{\mathbf{e}}_z + [\bar{u}]\hat{\mathbf{e}}_x) \\ \mathbf{b} &= (\hat{\mathbf{e}}_z \times [\bar{u}]\hat{\mathbf{e}}_x) = [\bar{u}]\hat{\mathbf{e}}_y \\ \mathbf{p} &= \frac{1}{\sqrt{2}} (\hat{\mathbf{e}}_z - [\bar{u}]\hat{\mathbf{e}}_x) \end{aligned} \right\}$$

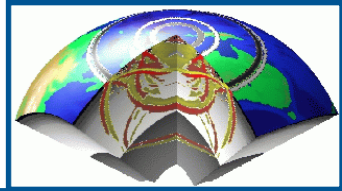


referred to principal axes

$$\mathbf{M} = \begin{pmatrix} M_0 & 0 & 0 \\ 0 & 0 & 0 \\ 0 & 0 & -M_0 \end{pmatrix}$$



GF for moment tensor



We can calculate the radiation pattern from a point source with an arbitrary moment tensor by noting that Green's function for a couple is just the spatial derivative of Green's function for a point force, so that the **displacement field from a moment tensor M_{pq}** is just:

$$u_n = M_{pq} * G_{np,q} = \lim_{\substack{\Delta l_q \rightarrow 0 \\ F_p \rightarrow \infty}} \Delta l_q F_p * \frac{\partial G_{np}}{\partial \zeta_q} =$$

$$= \frac{u^{NF}}{4\pi\rho} \int_{|x|/\alpha}^{|x|/\beta} \tau M_{pq}(t-\tau) d\tau +$$

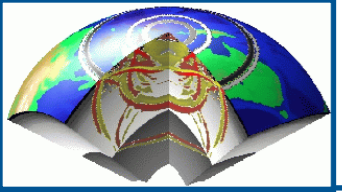
Near field term

$$+ \frac{u_p^{IF}}{4\pi\rho\alpha^2} M_{pq}\left(t - \frac{|x|}{\alpha}\right) - \frac{u_s^{IF}}{4\pi\rho\beta^2} M_{pq}\left(t - \frac{|x|}{\beta}\right) +$$

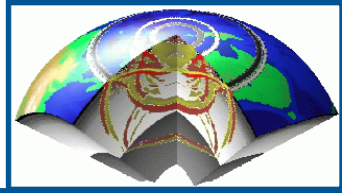
Intermediate field term

$$+ \frac{u_p^{FF}}{4\pi\rho\alpha^3} \dot{M}_{pq}\left(t - \frac{|x|}{\alpha}\right) - \frac{u_s^{FF}}{4\pi\rho\beta^3} \dot{M}_{pq}\left(t - \frac{|x|}{\beta}\right)$$

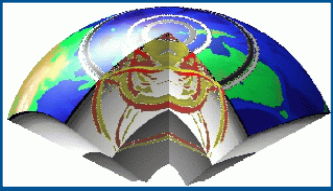
Far field term



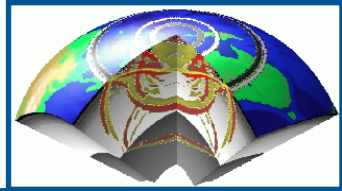
Faulting and Seismograms



- The nature of faulting affects the amplitudes and shapes of seismic waves (this allows us to use seismograms to study the faulting).
- We call the variation in wave amplitude, due to the source, with direction (i.e. angular) the **radiation pattern**.



Far field for a point DC point source



From the representation theorem we have: $u_n(\mathbf{x}, t) = M_{pq} * G_{np,q}$
 that, in the far field and in a spherical coordinate system becomes:

$$u(\mathbf{x}, t) = \frac{1}{4\pi\rho\alpha^3} (\sin 2\theta \cos \phi \hat{r}) \frac{\dot{M}(t - r/\alpha)}{r} +$$

$$\frac{1}{4\pi\rho\beta^3} (\cos 2\theta \cos \phi \hat{\theta} - \cos \theta \sin \phi \hat{\phi}) \frac{\dot{M}(t - r/\beta)}{r}$$

and both P and S radiation fields are proportional to the time derivative of the moment function (moment rate). If the moment function is a ramp of duration τ (**rise time**), the propagating disturbance in the far-field will be a **boxcar**, with the same duration, and whose amplitude is varying depending on the radiation pattern.

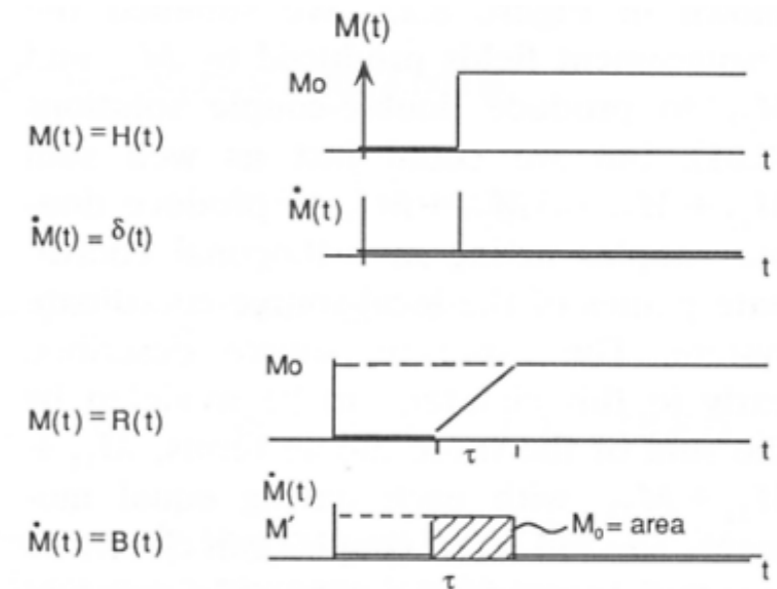
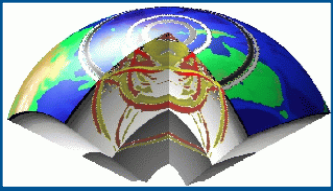
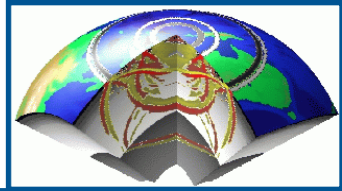


FIGURE 8.21 Far-field P- and S-wave displacements are proportional to $\dot{M}(t)$, the time derivative of the moment function $M(t) = \mu A(t)D(t)$. Simple step and ramp moment functions generate far-field impulses or boxcar ground motions.



P-waves RP



P-wave radiation amplitude patterns:

$$u_r = \frac{1}{4\pi\rho\alpha^3r} \dot{M}(t - r/\alpha) \sin 2\theta \cos \phi.$$

$\frac{1}{4\pi\rho\alpha^3r}$ = amplitude term, with geometric spreading

$\sin 2\theta \cos \phi$ = P-wave radiation pattern (4-lobed)

$\dot{M}(t - r/\alpha)$ = source time function

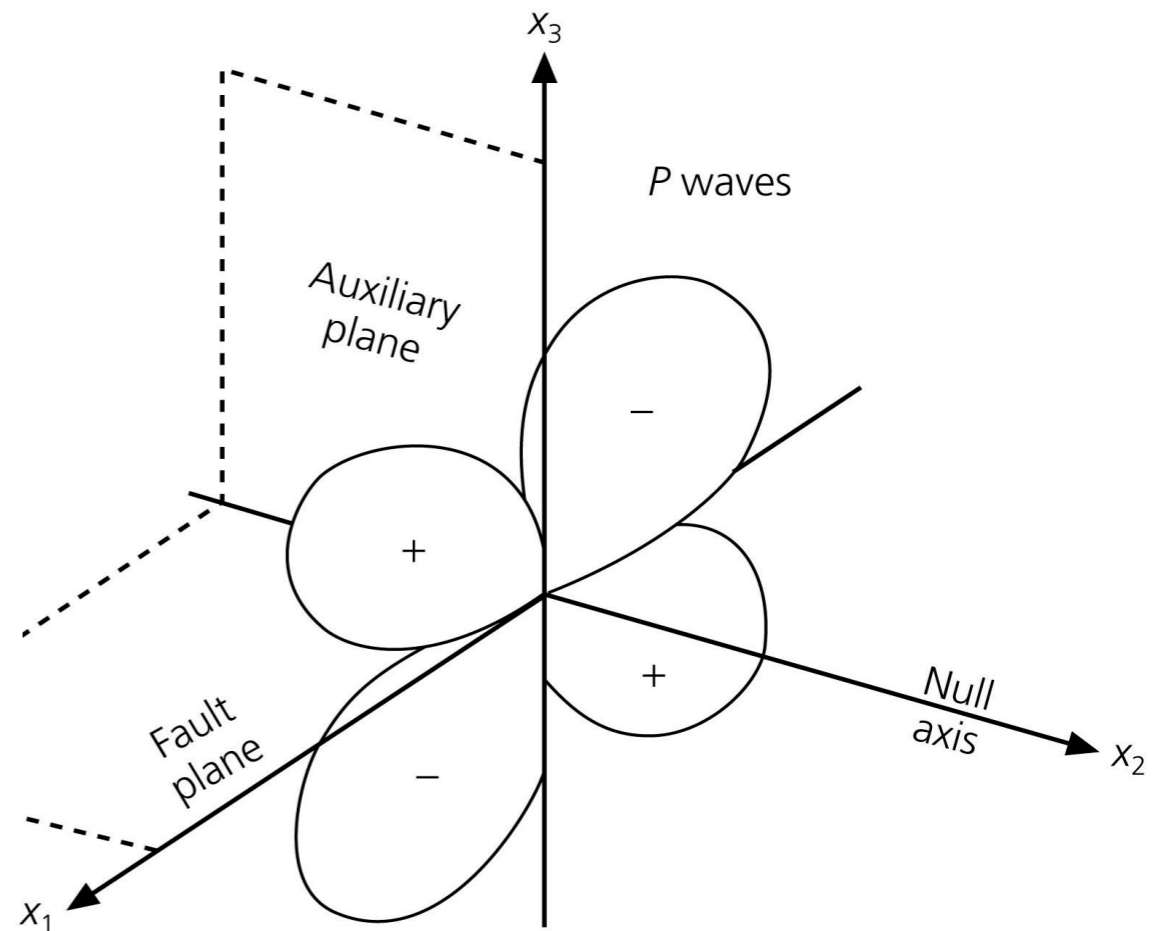
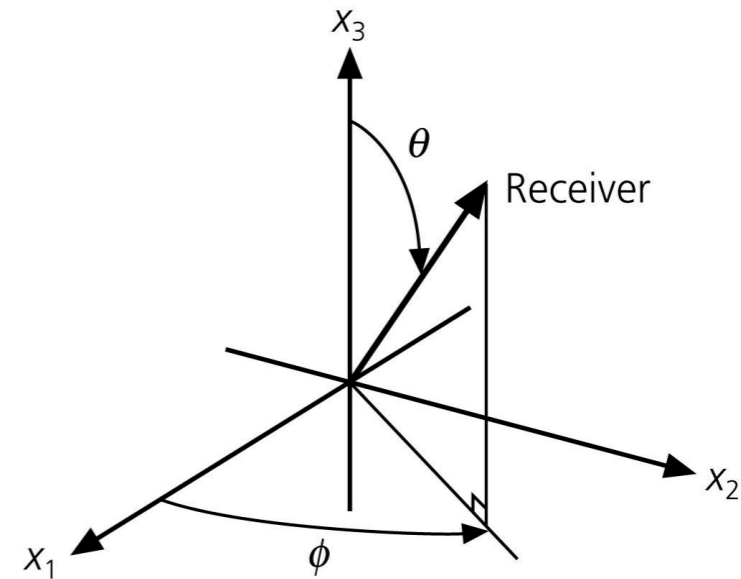
\dot{M} is the time derivative of the seismic moment function,

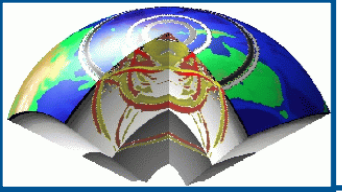
$$M(t) = \mu D(t) S(t)$$

$D(t)$ = slip history

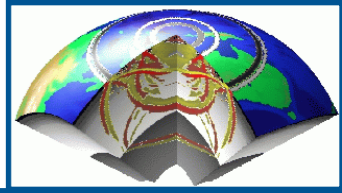
$S(t)$ = fault area history

Body-wave radiation patterns for a double couple source.





S-waves RP



S-wave radiation amplitude patterns:

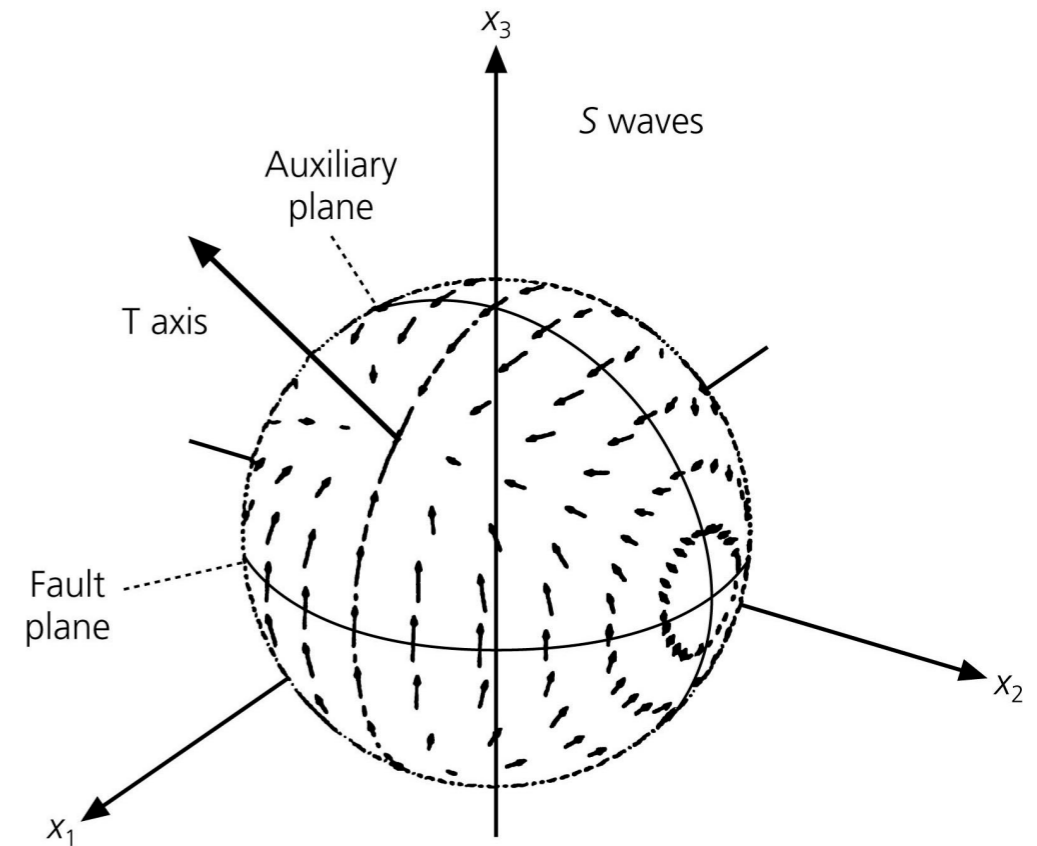
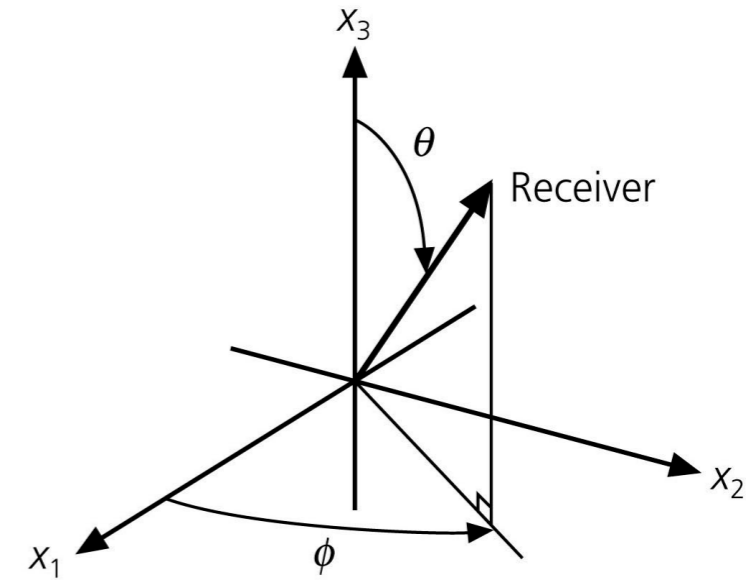
$$u_{\theta} = \frac{1}{4\pi\rho\beta^3r} \dot{M}(t - r/\beta) \cos 2\theta \cos \phi$$

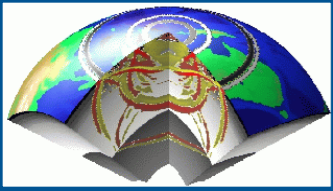
$$u_{\phi} = \frac{1}{4\pi\rho\beta^3r} \dot{M}(t - r/\beta) (-\cos \theta \sin \phi)$$

Why are *S* waves usually larger than *P* waves?

These equations predict an average ratio of about α^3/β^3 or about 5.

Figure 4.2-6: Body-wave radiation patterns for a double couple source.





P&S waves RP

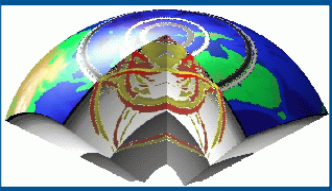
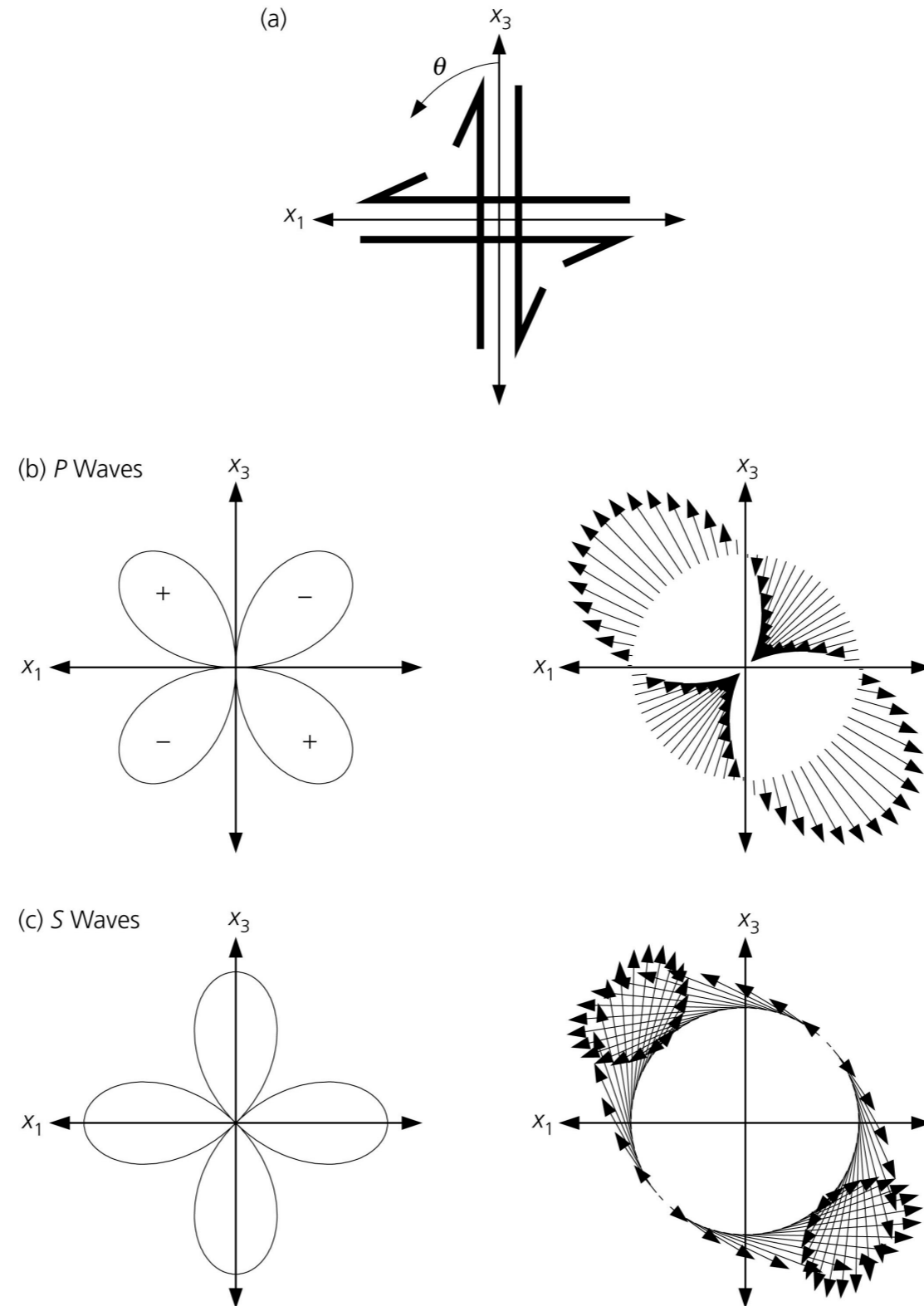
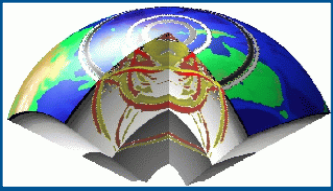
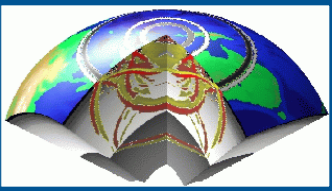


Figure 4.2-7: P and S radiation amplitude patterns.

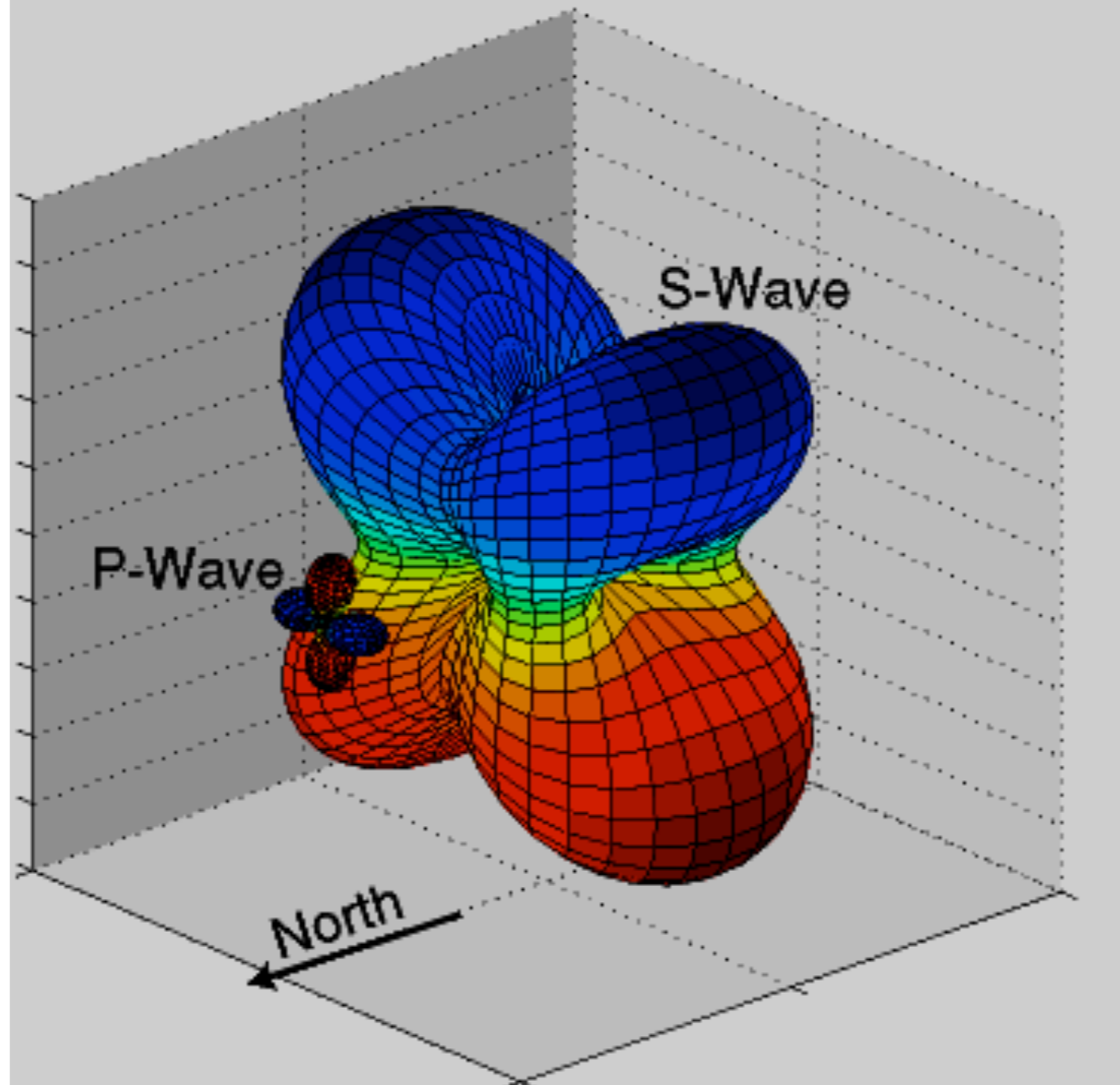




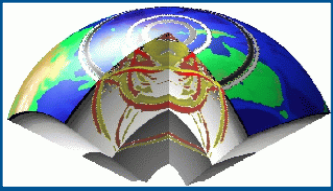
Radiation Patterns in 3D



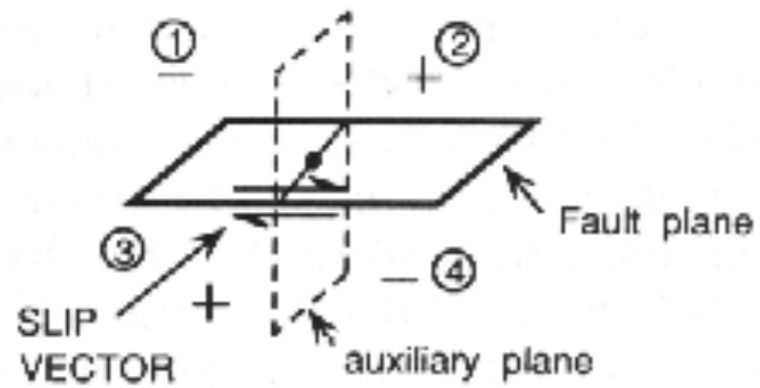
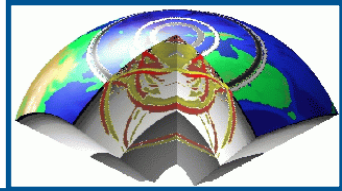
Radiation Patterns of P and S waves
for a 45° Dipping Fault with a Strike Due North



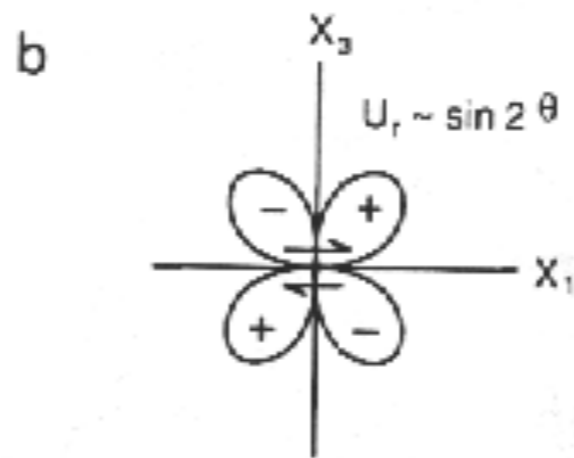
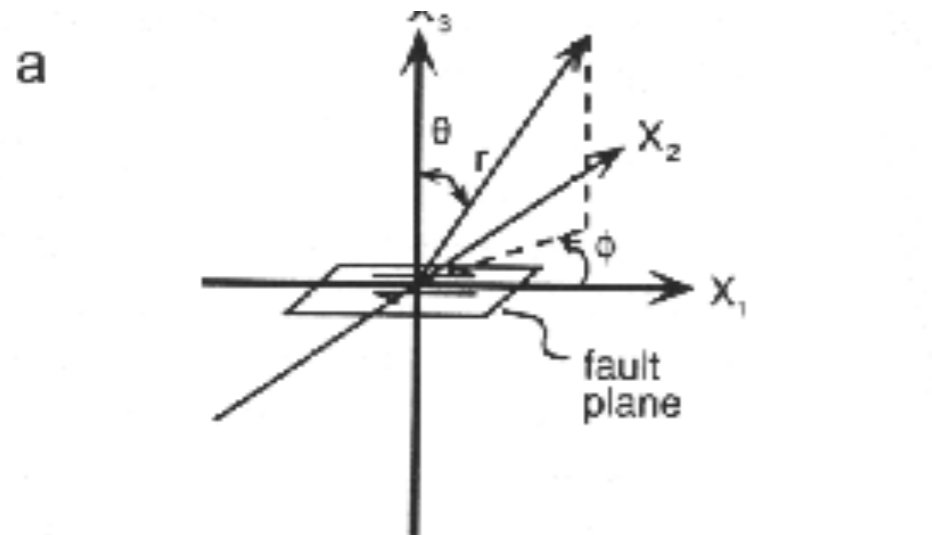
<http://demonstrations.wolfram.com/RadiationPatternForDoubleCoupleEarthquakeSources/>



Radiation from shear dislocation

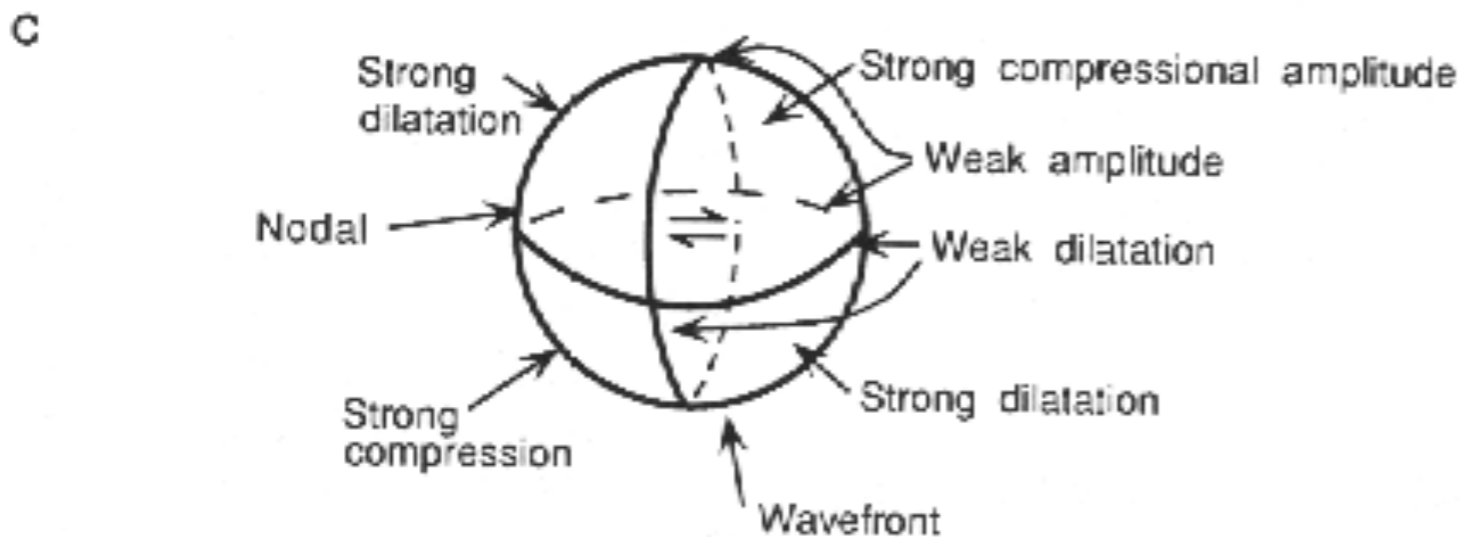


Fault plane and auxiliary plane and sense of initial P-wave motion.

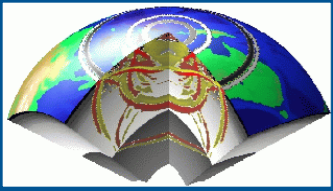


a) Coordinates parallel or perpendicular to fault plane with one axis along the slip direction.

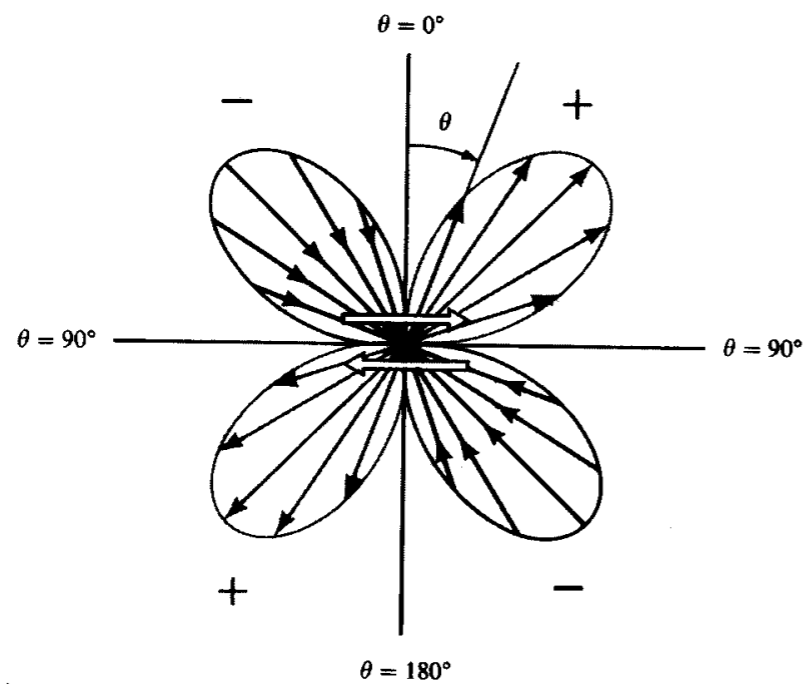
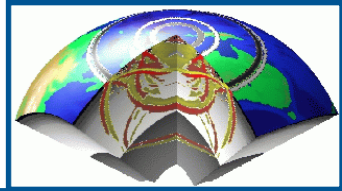
b) radiation pattern in x - z plane



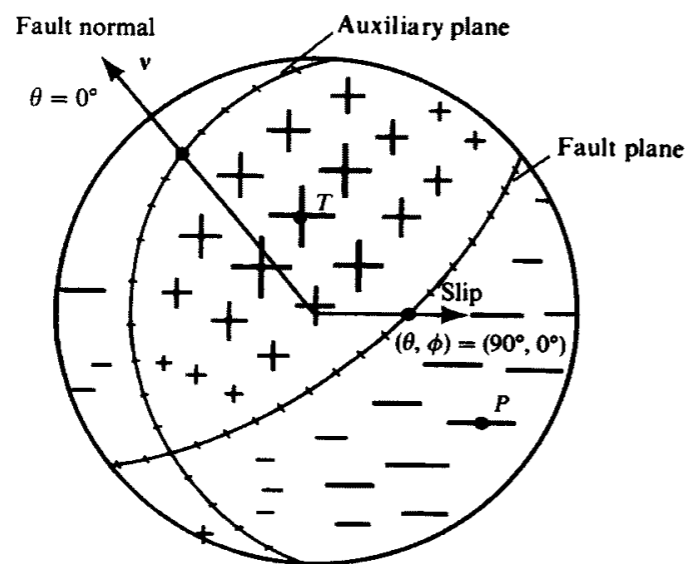
c) 3-D variation of P amplitude and polarity of wavefront from a shear dislocation



Double Couple radiation pattern - P waves



(a)



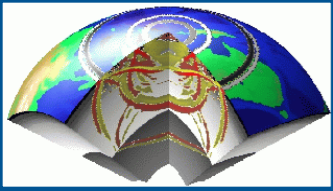
(b)

Radiation pattern of the radial displacement component (P-wave) due to a double-couple source:

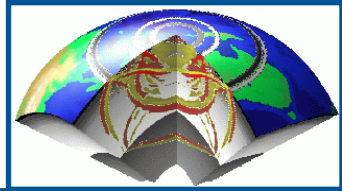
a) for a plane of constant azimuth (with lobe amplitudes proportional to $\sin 2\theta$). The pair of arrows at the center denotes the shear dislocation.

b) over the focal sphere centered on the origin. Plus and minus signs of various sizes denote amplitude variation (with θ and φ) of outward and inward directed motions. The fault plane and auxiliary plane are nodal lines on which $\cos \varphi \sin 2\theta = 0$.

Note the alternating quadrants of inward and outward directions.



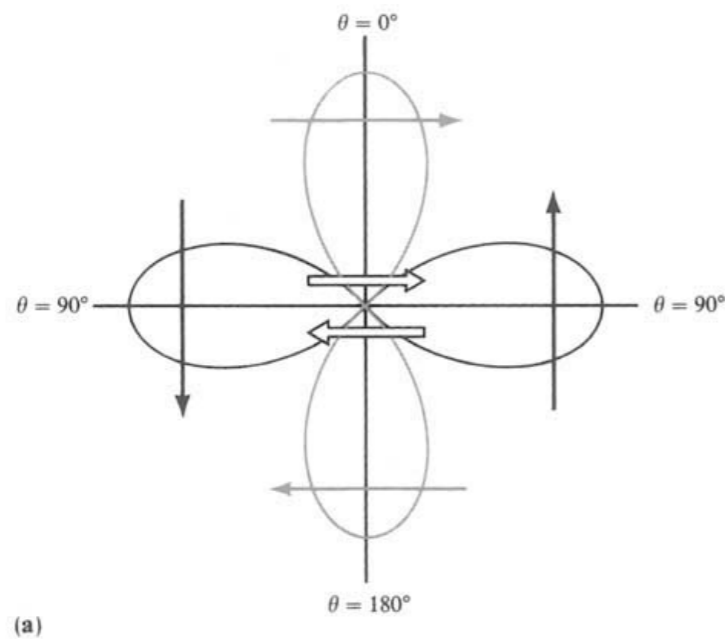
Double Couple radiation pattern - S waves



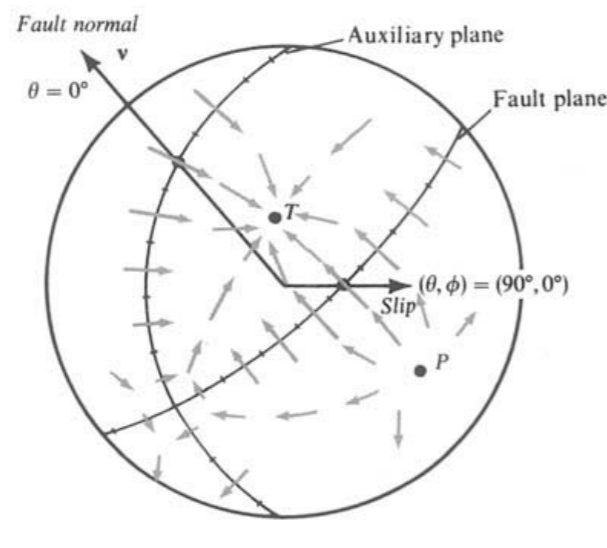
Radiation pattern of the transverse displacement component (S-wave) due to a double-couple source:

a) in the plane $\{ \varphi = 0, \varphi = \pi \}$.

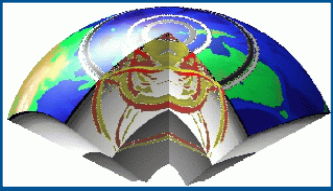
Arrows imposed on each lobe show the direction of particle displacement; the pair of arrows in a) at the center denotes the shear dislocation



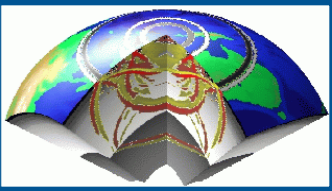
b) over a sphere centered on the origin. Arrows with varying size and direction indicate the variation of the transverse motions with θ and φ . There are no nodal lines but only nodal points where there is zero motion.



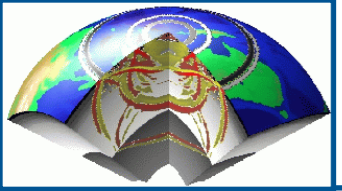
Note that the nodal point for transverse motion at $(\theta, \varphi) = (45^\circ, 0^\circ)$ at T is a maximum in the pattern for longitudinal motion while the maximum transverse motion (e.g. at $\theta = 0$) occurs on a nodal line for the longitudinal motion.



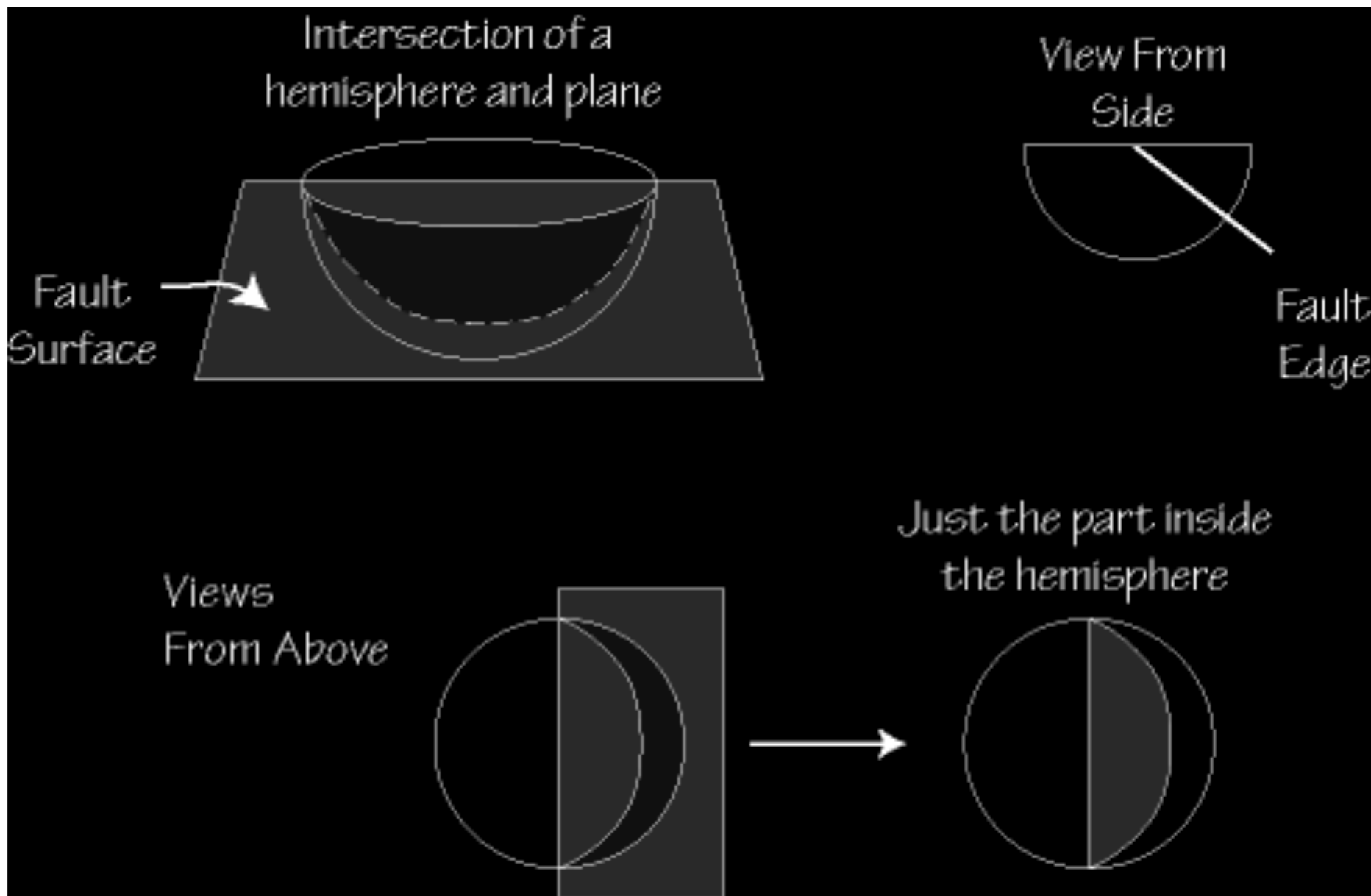
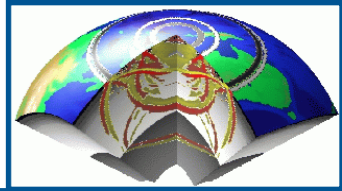
Seismic “Beach Balls”

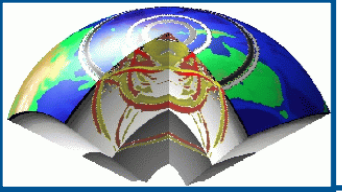


- We use the radiation patterns of P-waves to construct a graphical representation of earthquake faulting geometry.
- The symbols are called “Focal Mechanisms” or “Beach Balls”, and they contain information on the fault orientation and the direction of slip.
- They are:
 - Graphical shorthand for a specific faulting process (strike, dip, slip)
 - Projections of a sphere onto a circle (the lower focal hemisphere)
 - Representations of the first motion of seismic waves.
- When mapping the focal sphere to a circle (beachball) two things happen:
 - Lines (vectors) become points
 - Planes become curved lines

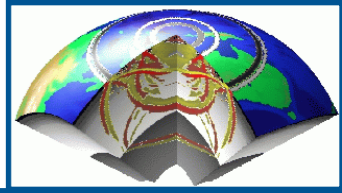


Representing a Plane

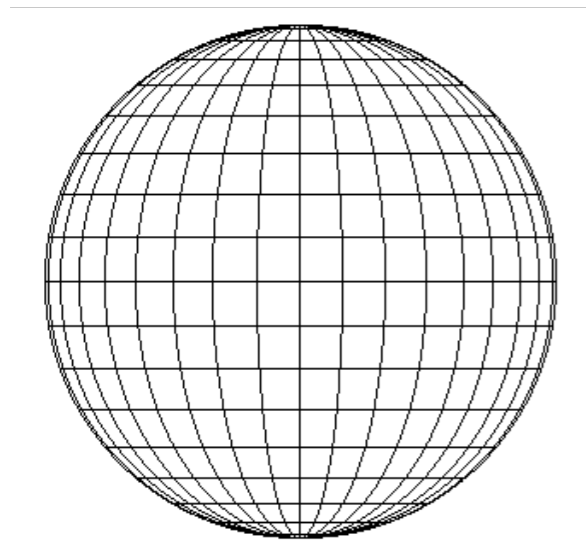




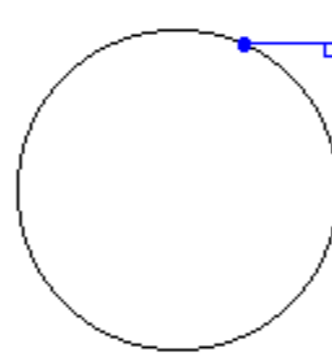
Two steps to understanding



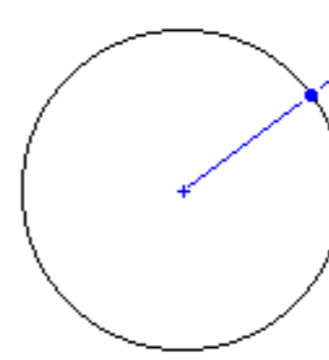
- 1) The stereographic projection
- 2) The geometry of first motions and how this is used to define fault motion.



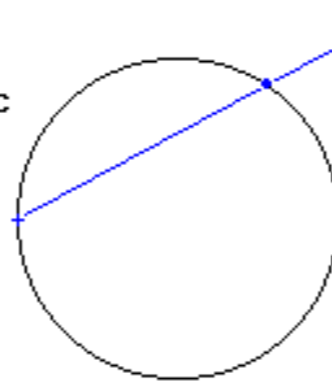
Orthographic



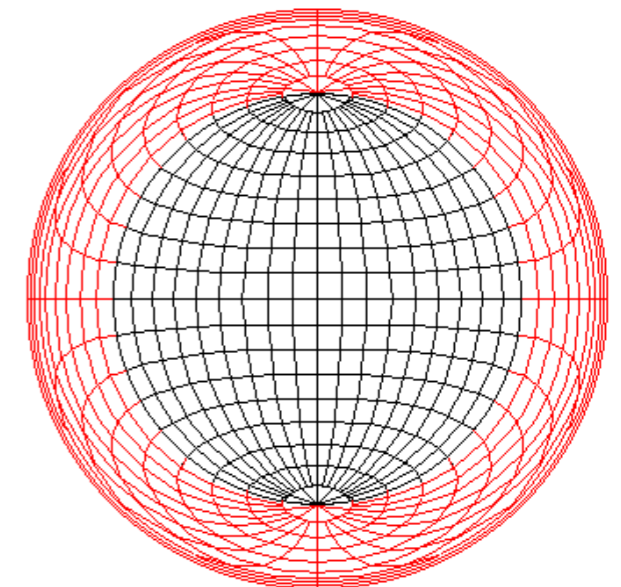
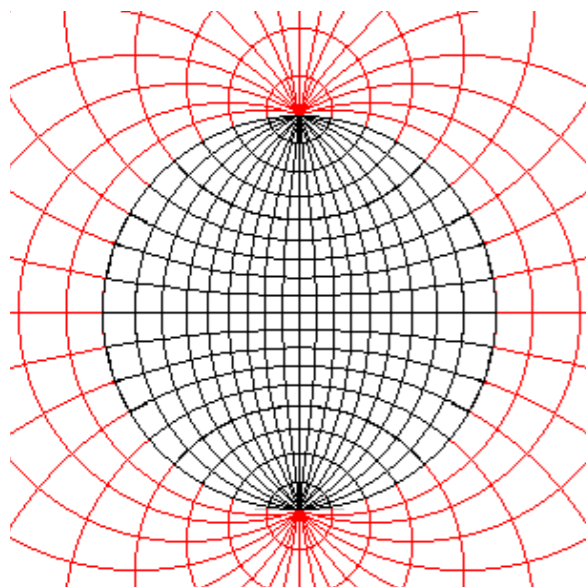
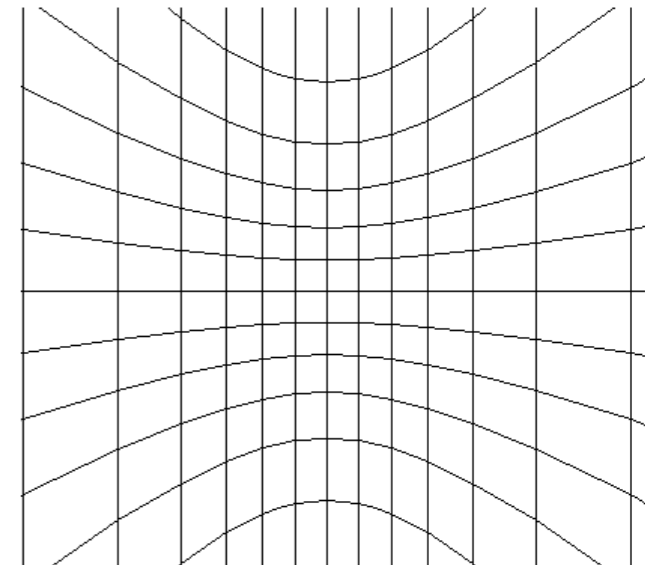
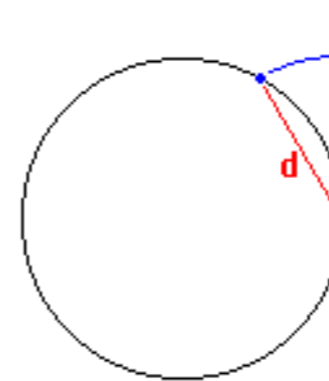
Gnomonic

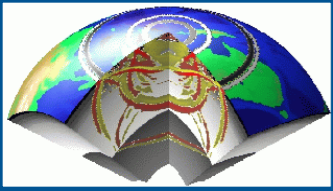


Stereographic

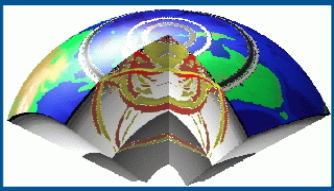


Equal-Area



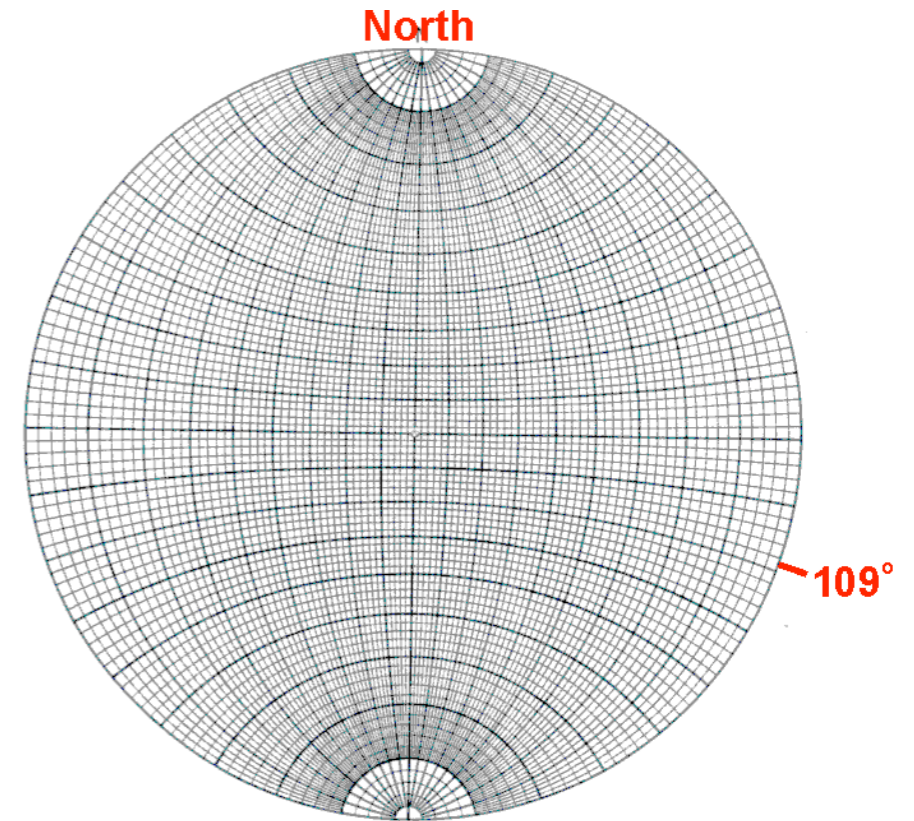
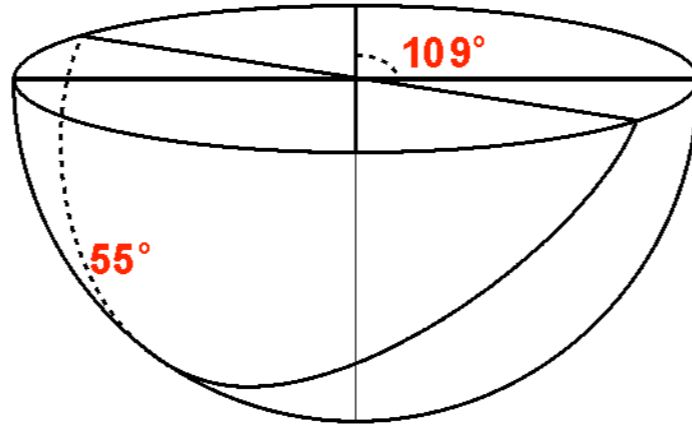


Stereonet

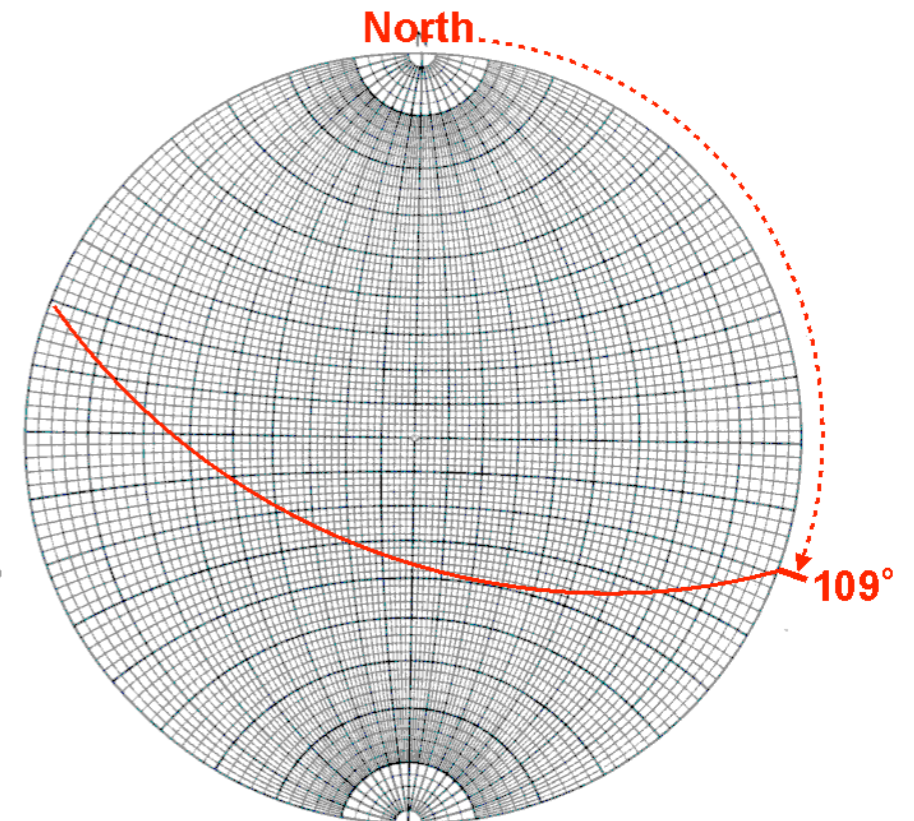
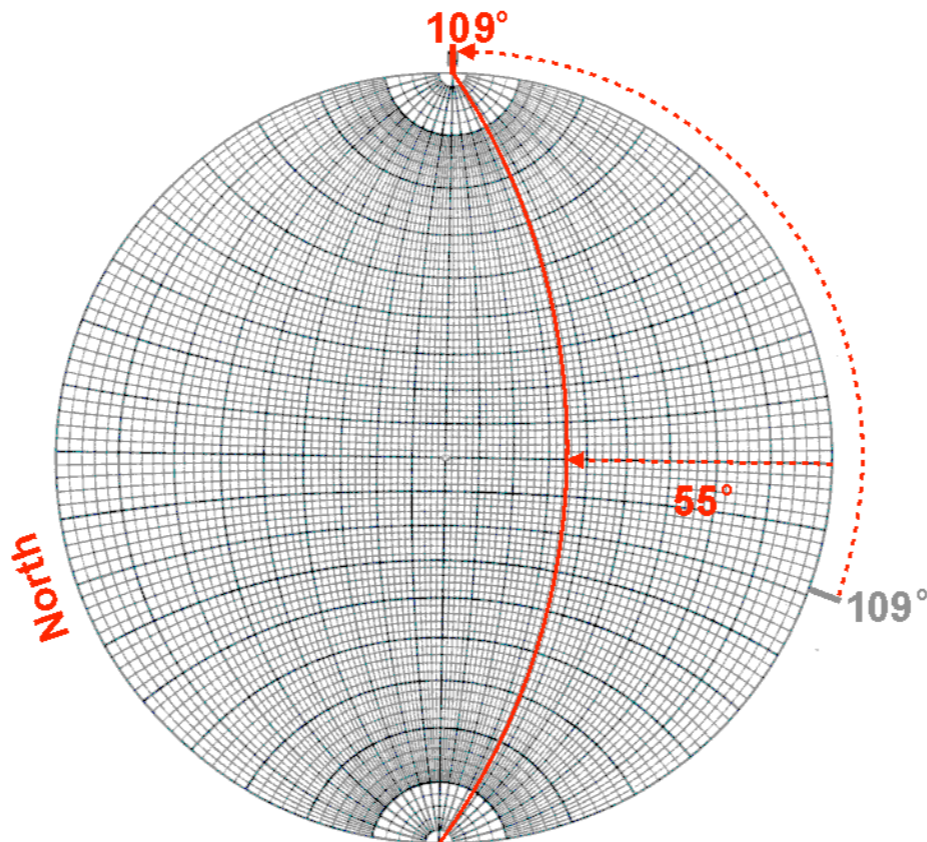


- A template called a stereonet is used to plot data.

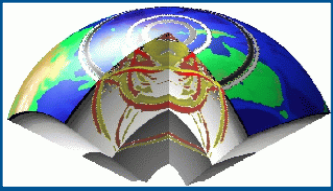
Fault strike 109° dip 55° SW



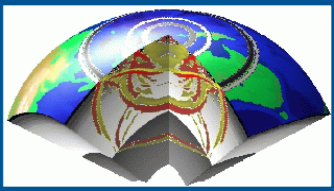
- Example - plotting planes (e.g. faults)



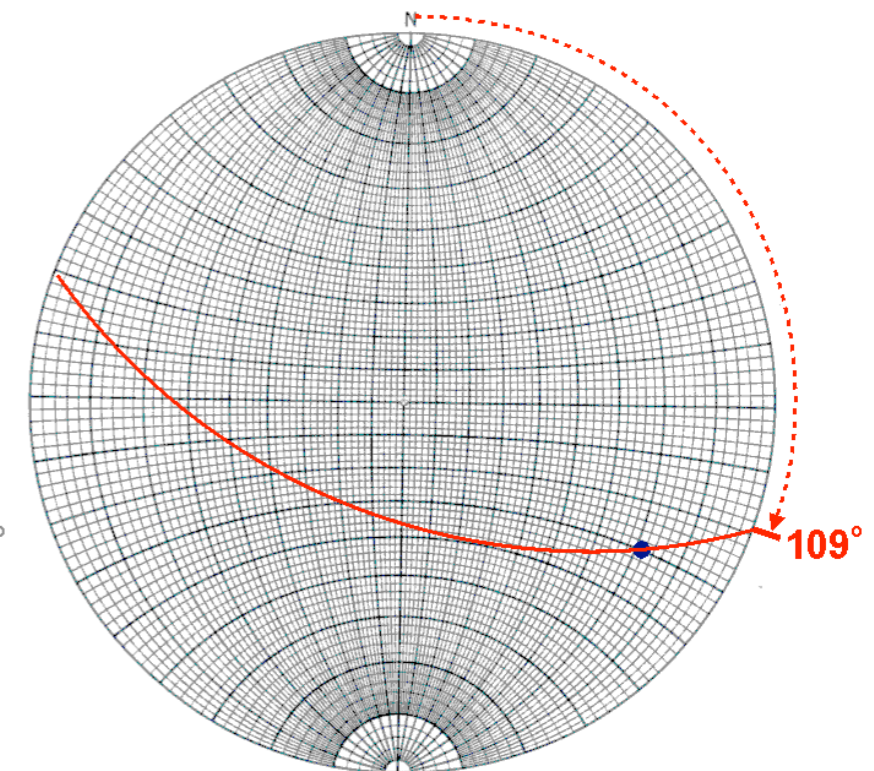
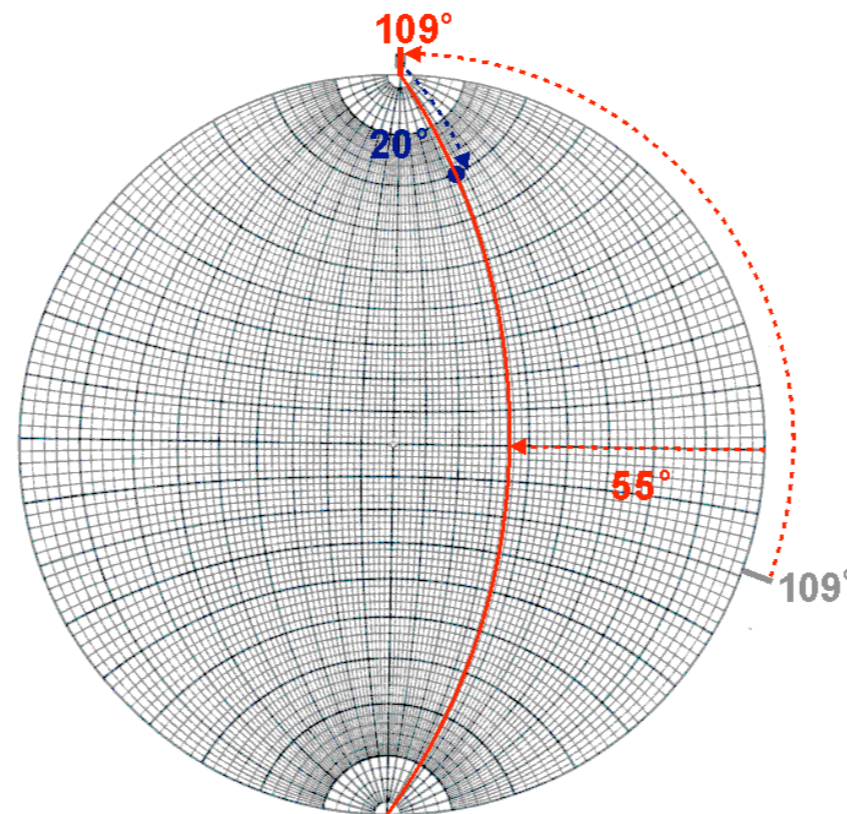
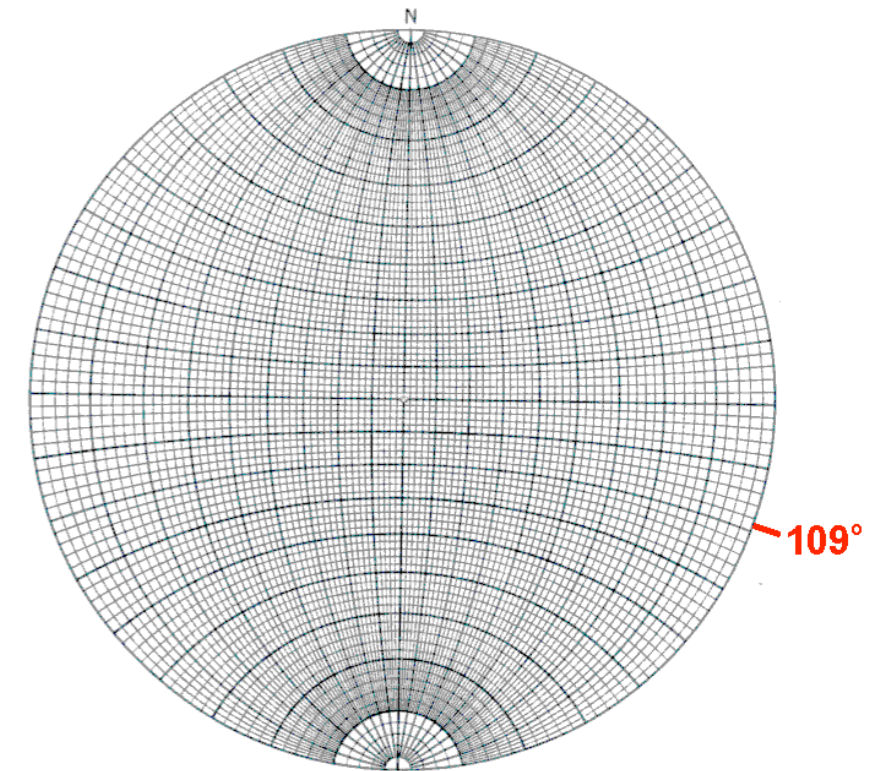
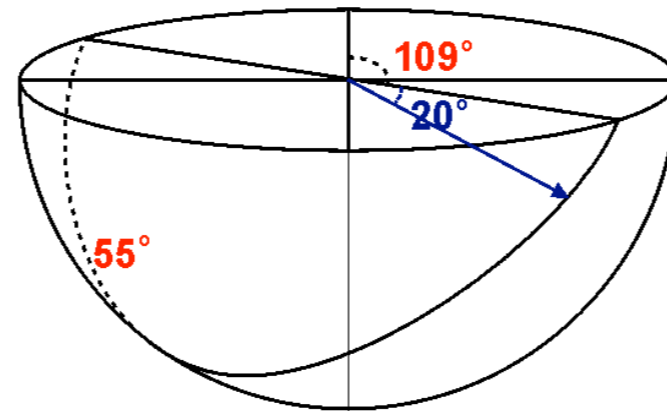
Source:USGS



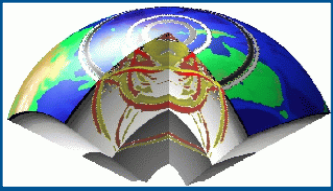
Stereonet



- Example – pitch (or rake) of a line on a plane (e.g. the slip direction on a fault)



Source:USGS



Stereonet

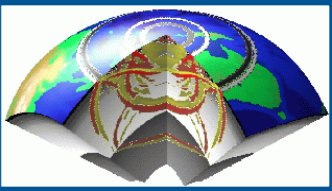
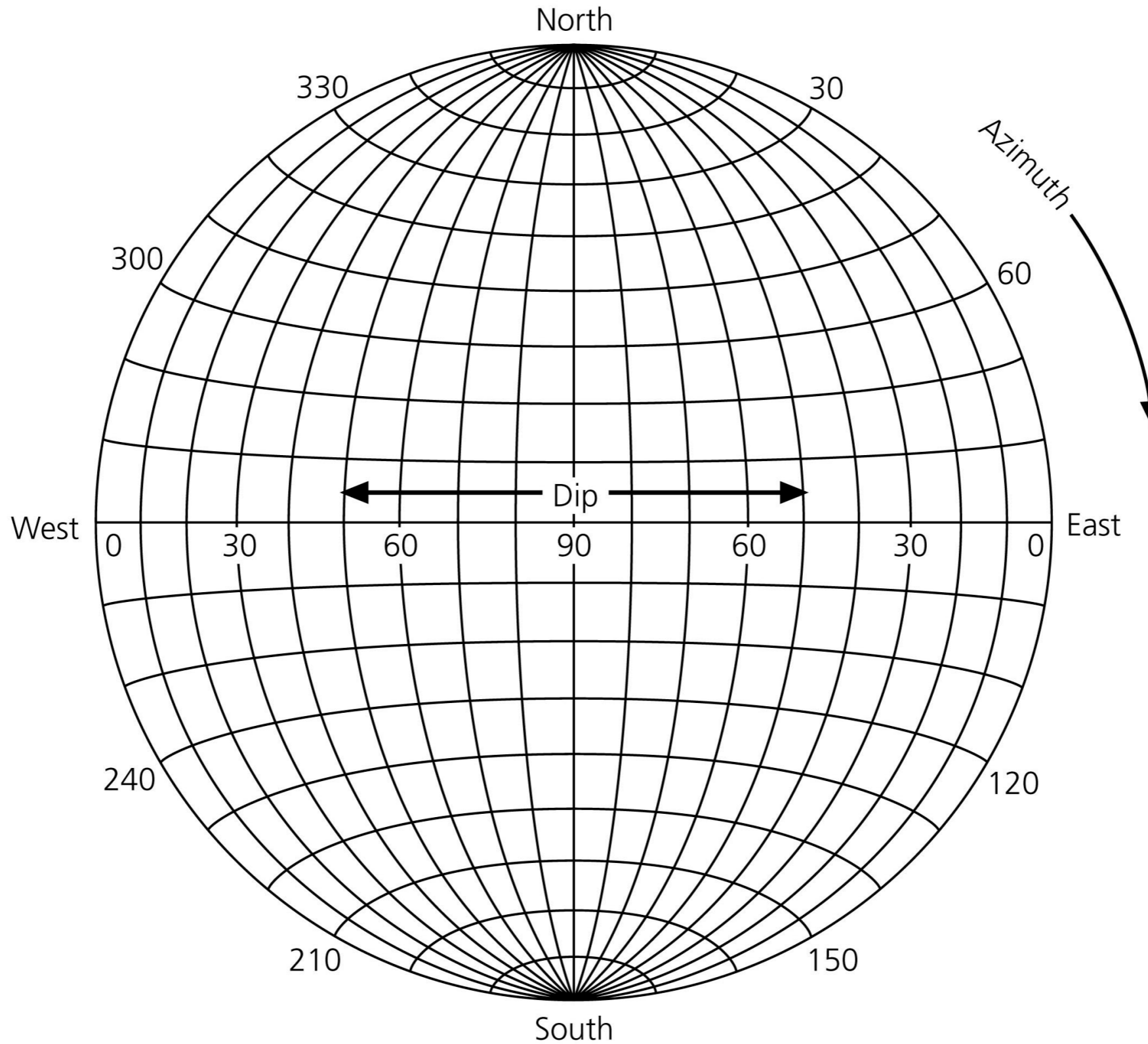
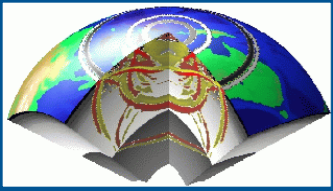


Figure 4.2-9: Stereonet used to display a hemisphere on a flat surface.





Stereonet - Dip

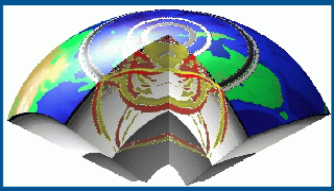
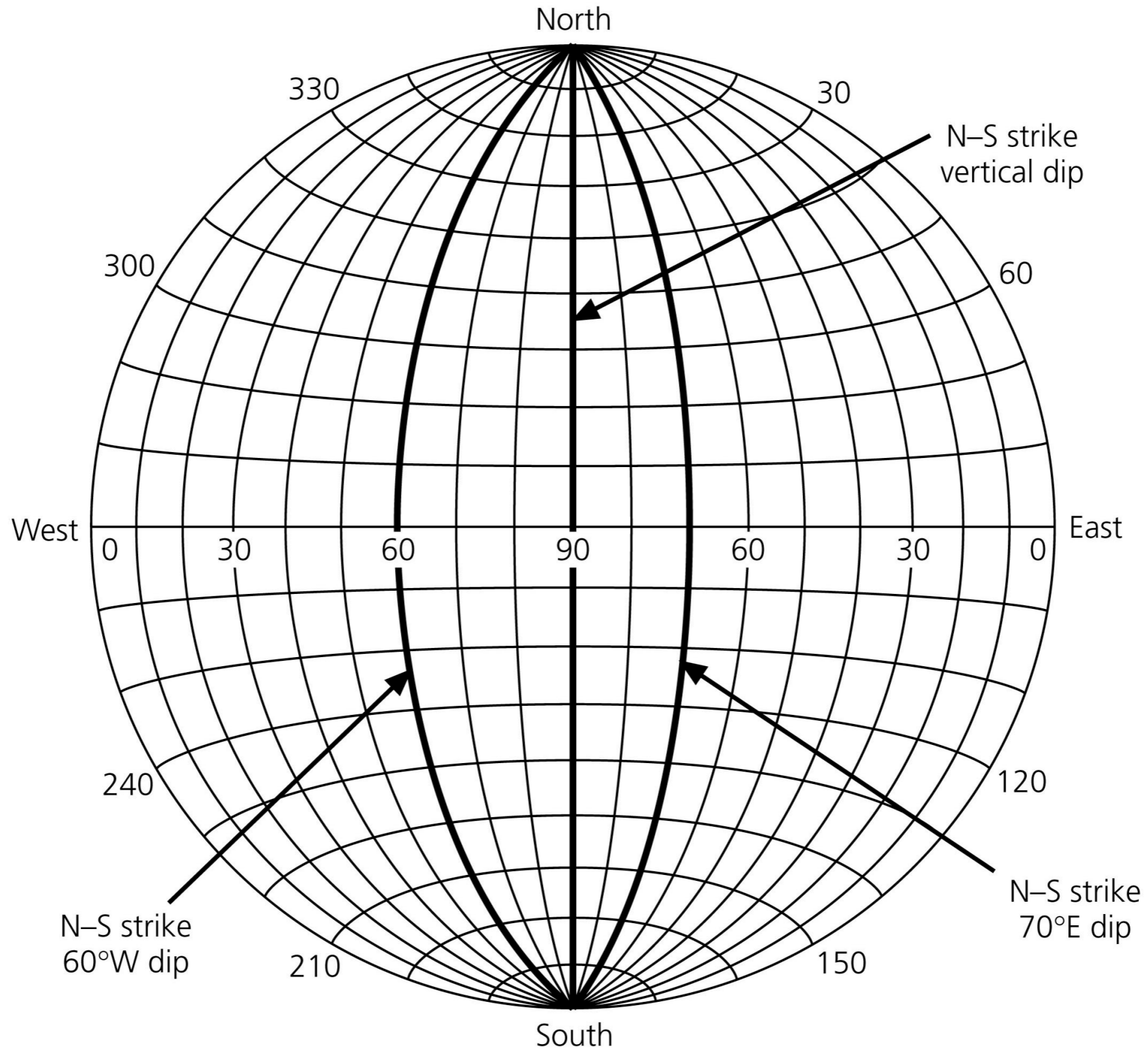
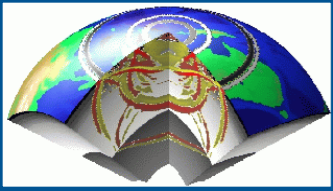


Figure 4.2-10: Example of three planes on a stereonet.





Stereonet - Plane

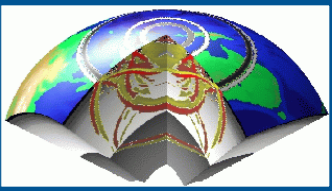
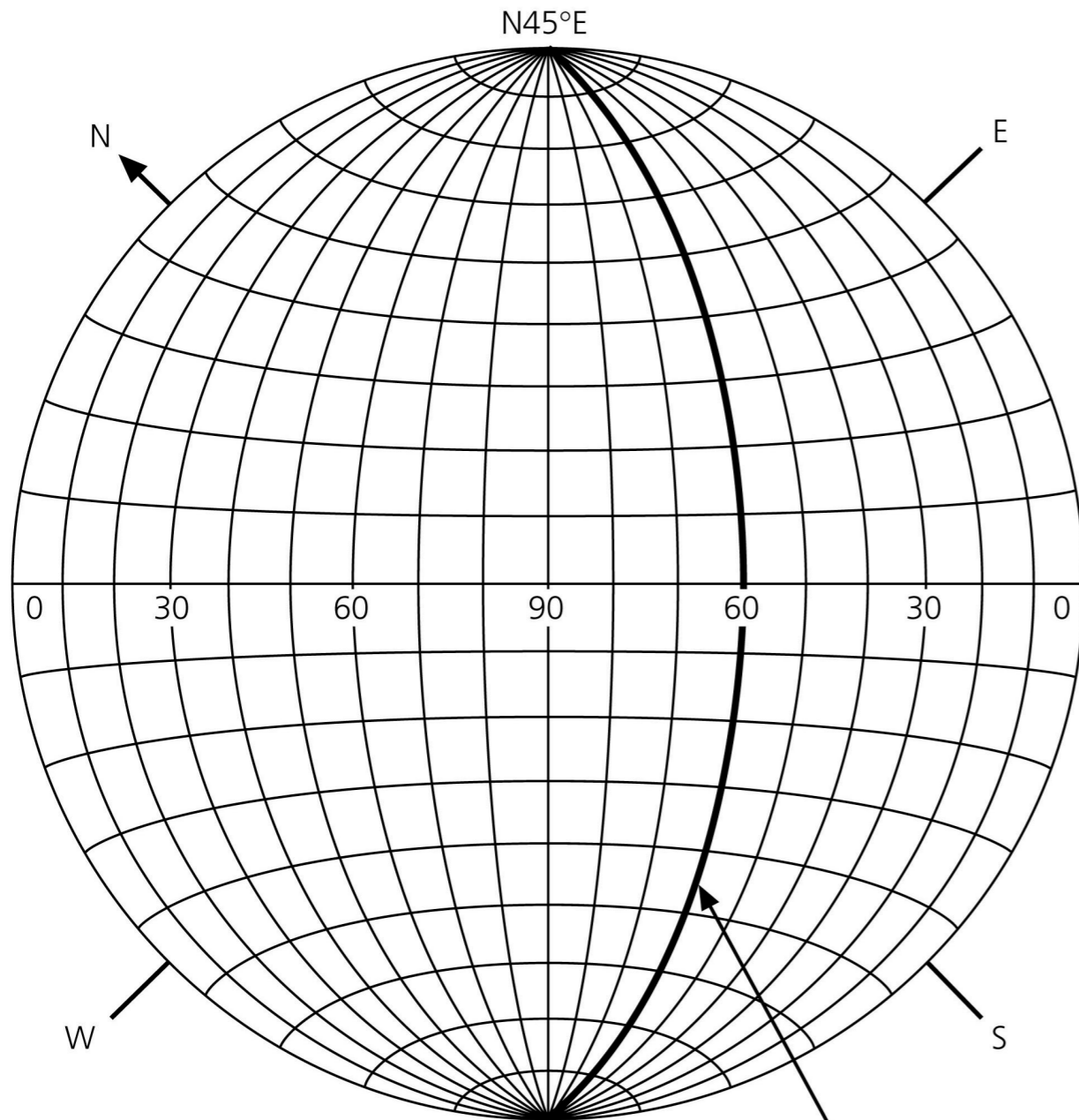
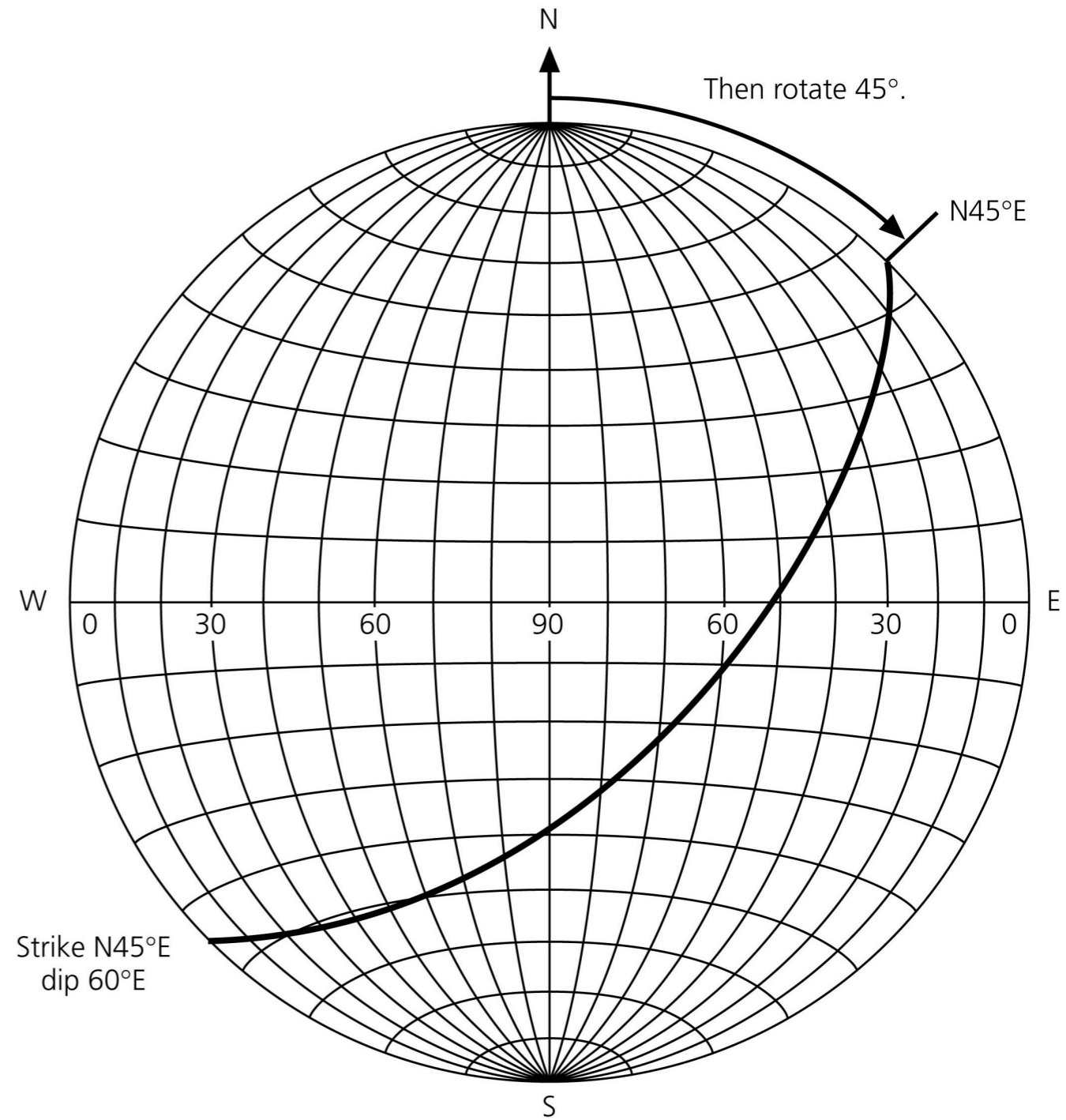
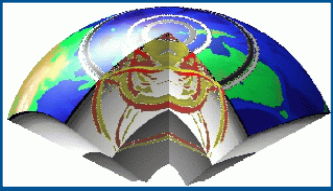


Figure 4.2-11: Example of plotting a plane on a stereonet.



First draw a plane with a dip of 60°E and a strike of 0°.





Stereonet - Planes

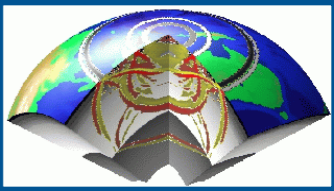
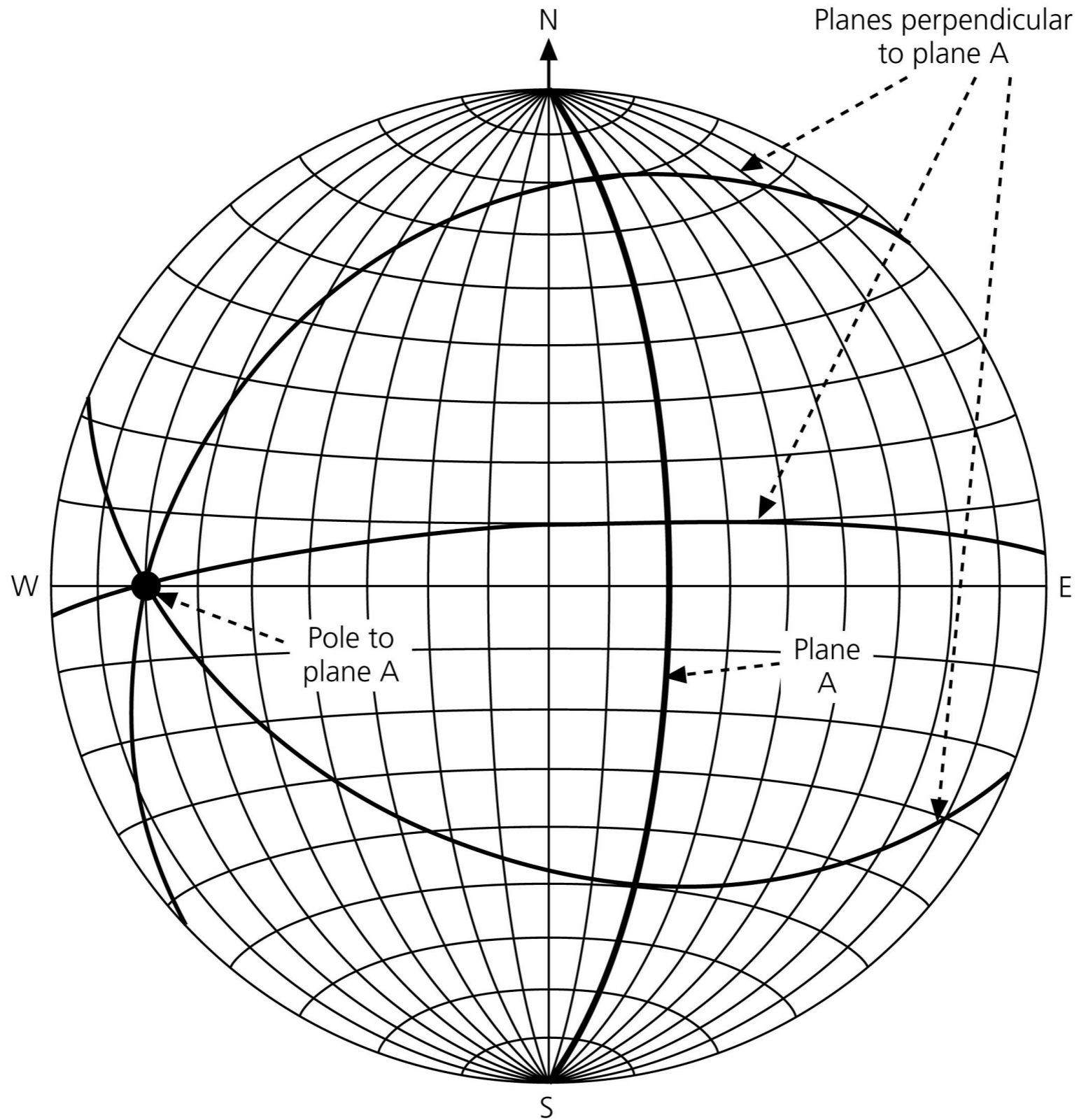
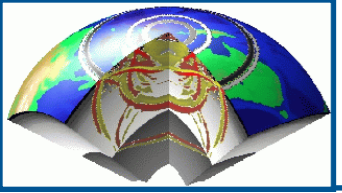
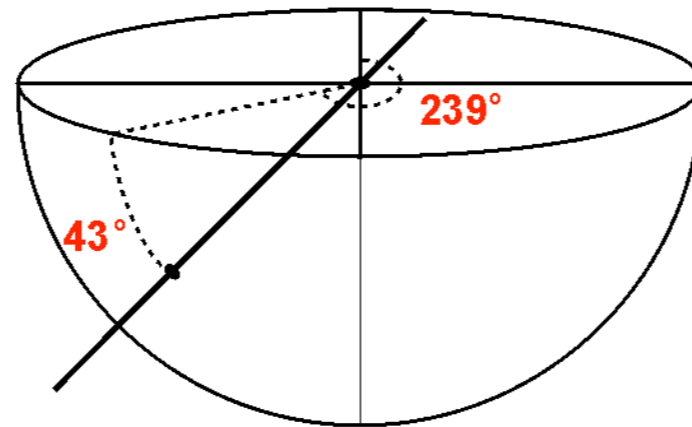
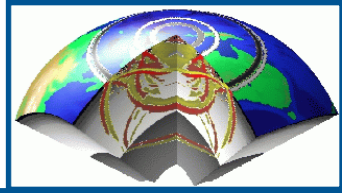


Figure 4.2-12: Example of plotting perpendicular planes on a stereonet.

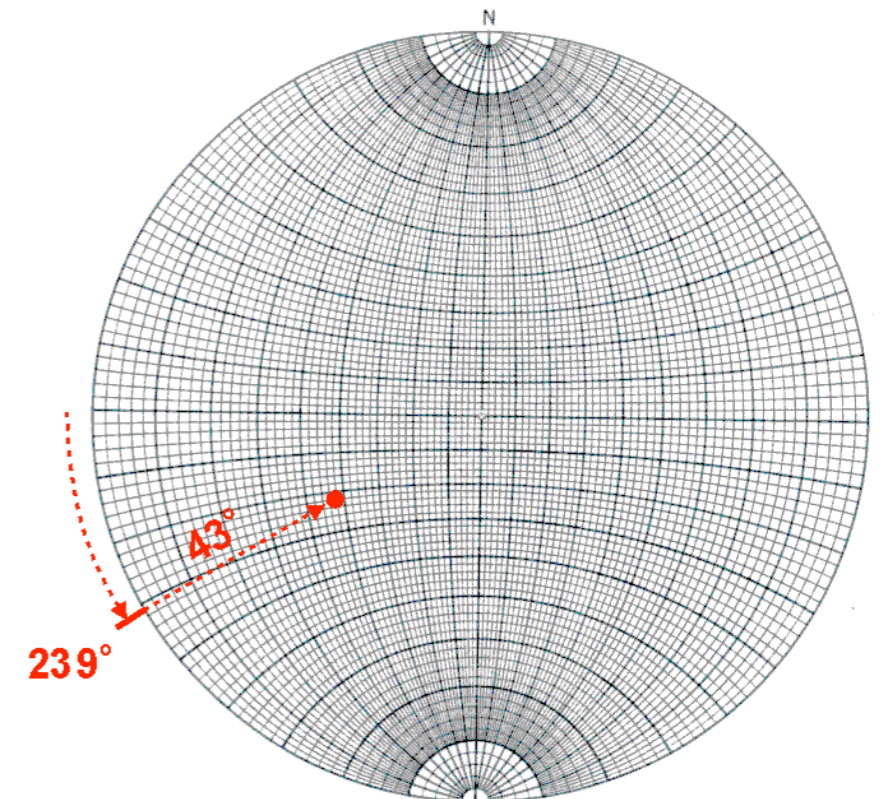
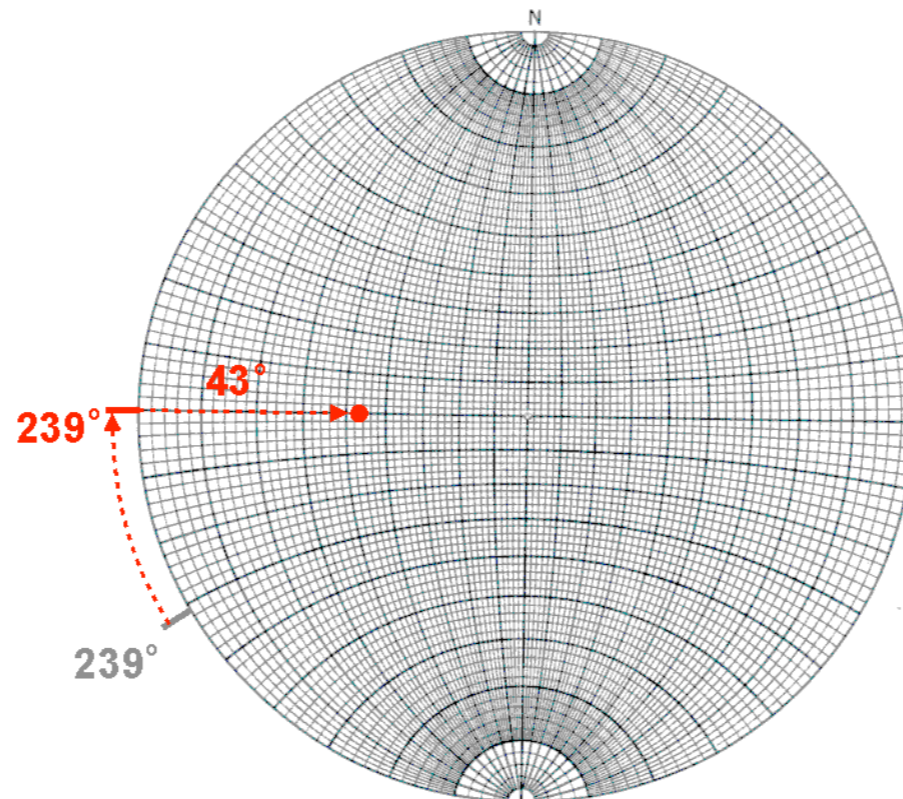
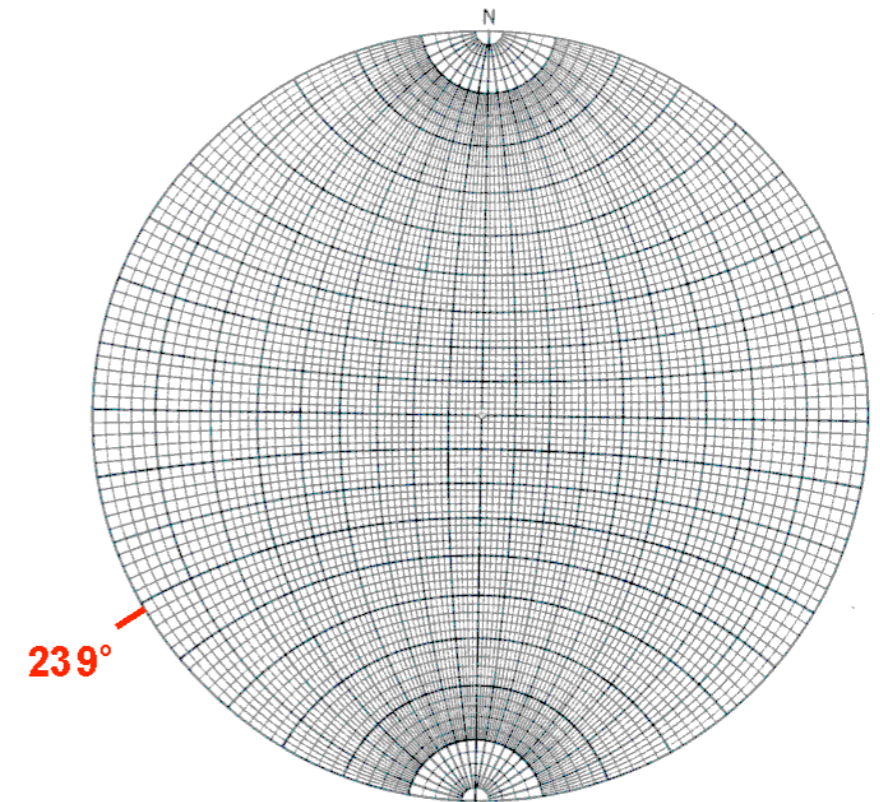




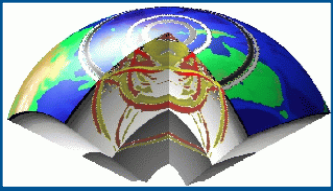
Stereonet - Rays



● Example - plotting lines (e.g. ray paths)



Source:USGS



Stereonet - Rays

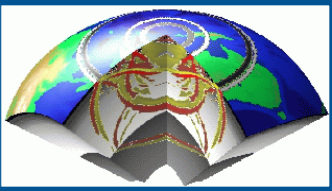
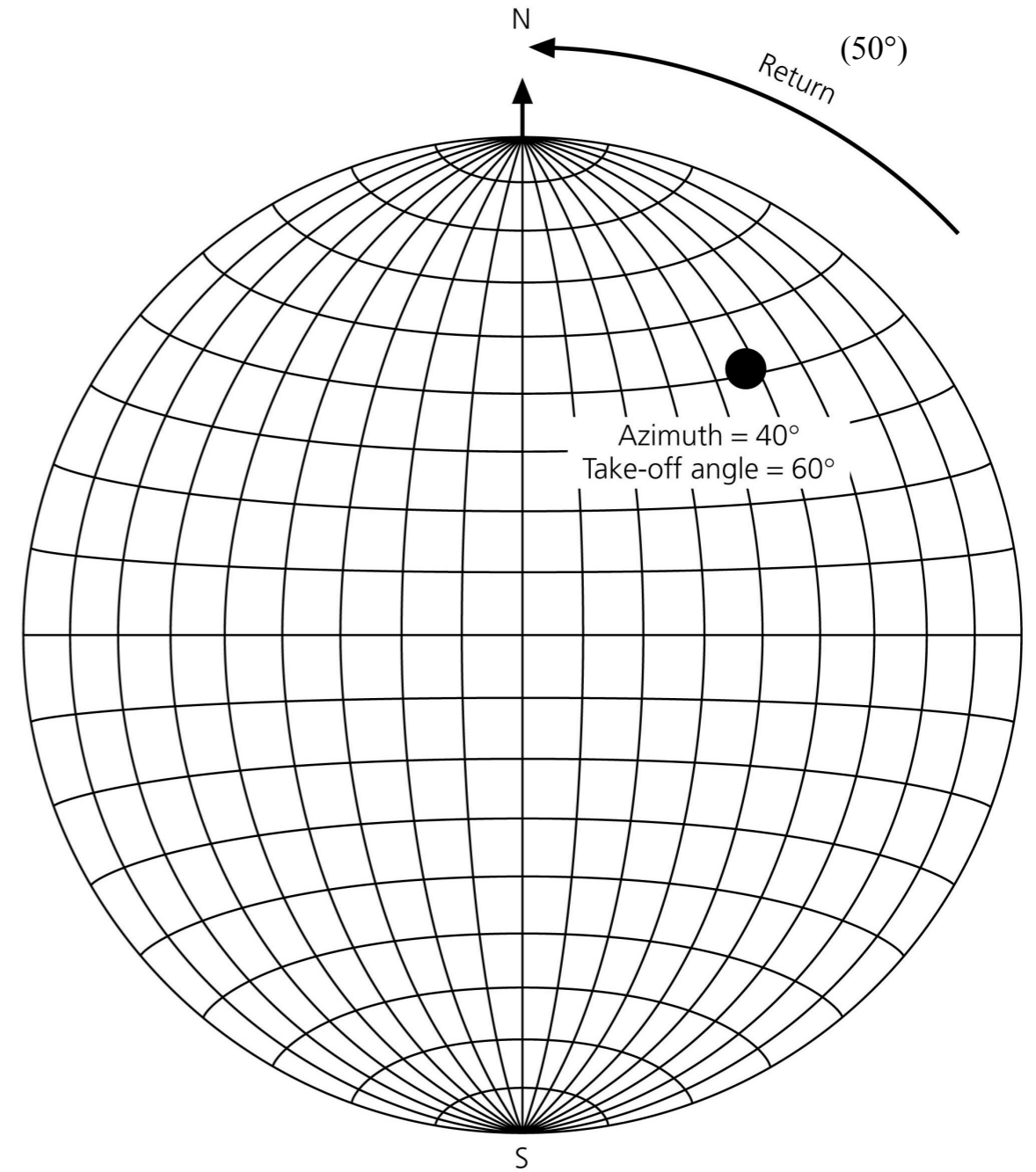
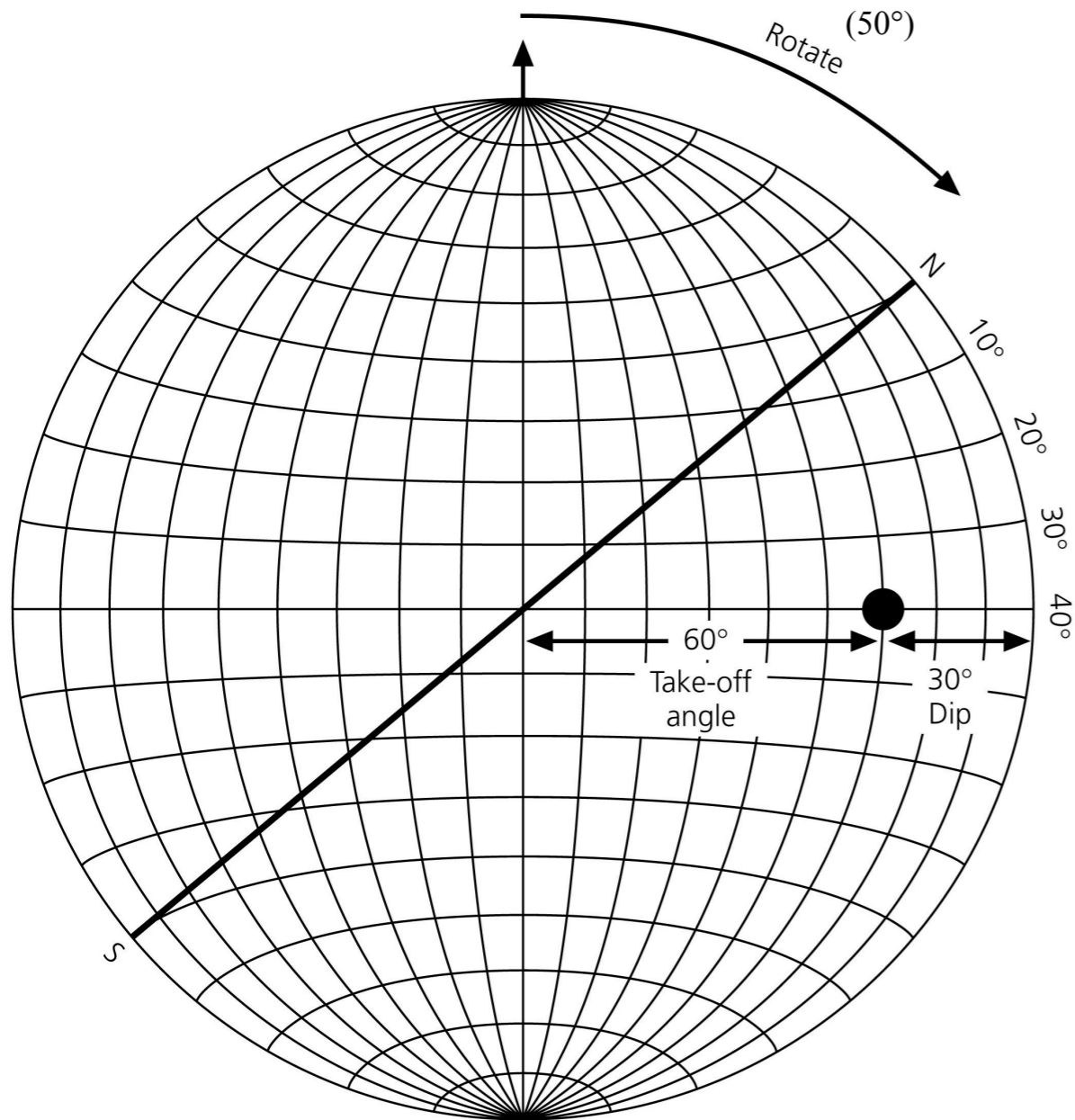
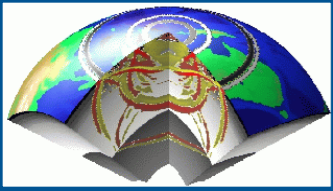
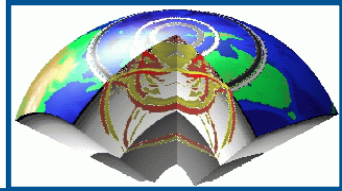


Figure 4.2-13: Plotting a ray on a stereonet.



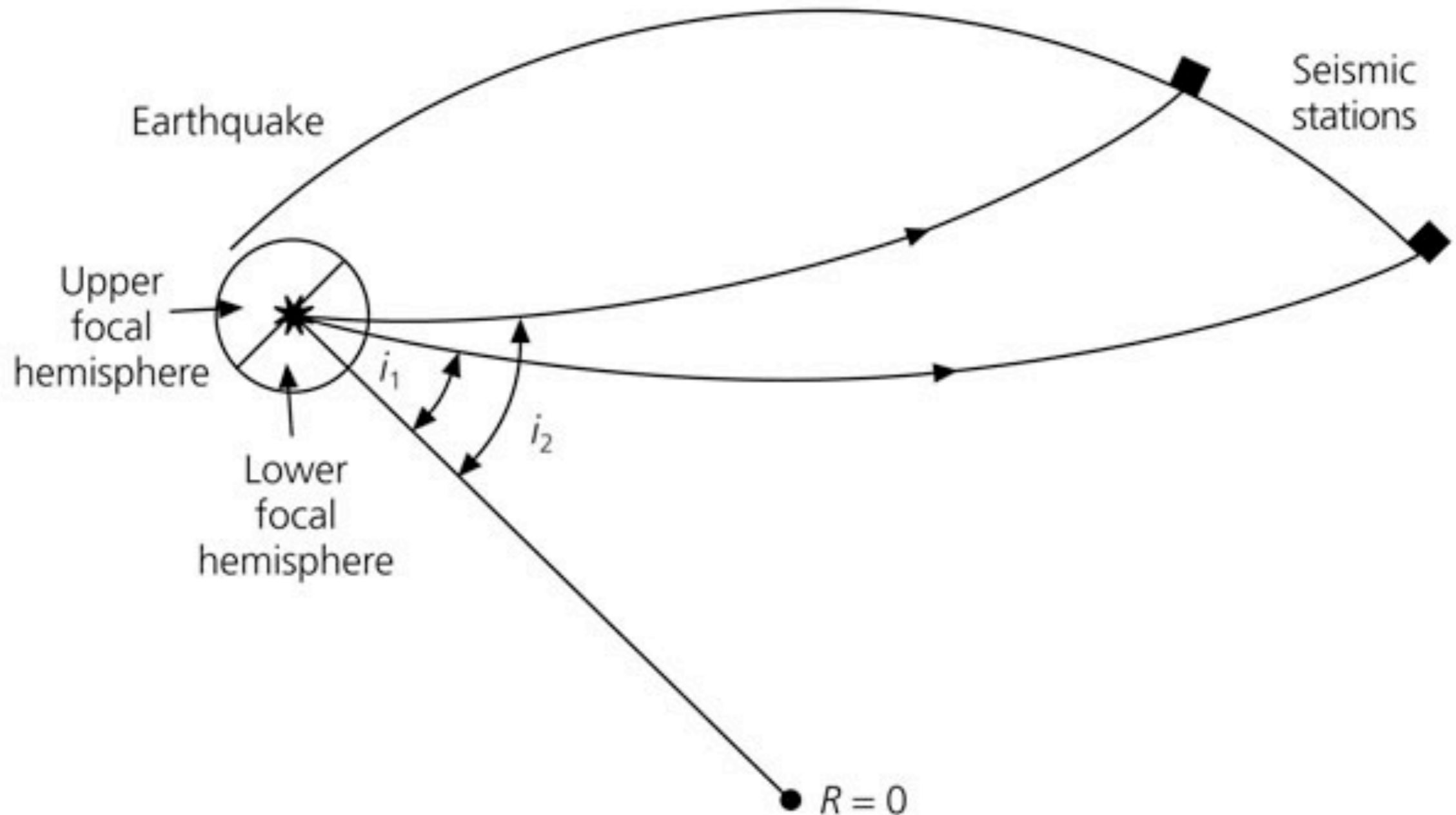


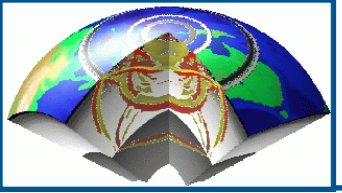
Focal sphere



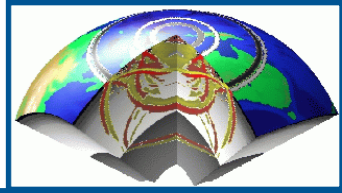
In order to simplify the analysis, the concept of the "focal sphere" is introduced. The focal sphere is an imaginary sphere drawn around the source region enclosing the fault. If we know the earthquake location and local Earth structure, we can trace rays from the source region to the stations and find the ray take-off angle at the source to a given station.

Figure 4.2-8: Cartoon of the focal sphere.





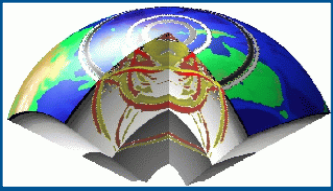
Take-off angle



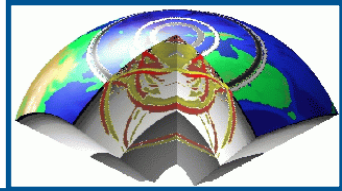
At a given source-receiver, the distance can be determined and from this T and the slope (p) can be found from the travel time tables. For example, the Jeffreys-Bullen travel time tables can be used to obtain p and from this the take-off angle i .

Table 4.2-1: P wave take-off angles for a surface focus earthquake.

Distance (°)	Take-off angle (°)	Distance (°)	Take-off angle (°)	Distance (°)	Take-off angle (°)
21	35	47	25	73	19
23	32	49	24	75	18
25	30	51	24	77	18
27	29	53	23	79	17
29	29	55	23	81	17
31	29	57	23	83	16
33	28	59	22	85	16
35	28	61	22	87	15
37	27	63	21	89	15
39	29	65	21	91	15
41	26	67	20	93	14
43	26	69	20	95	14
45	25	71	19	97	14

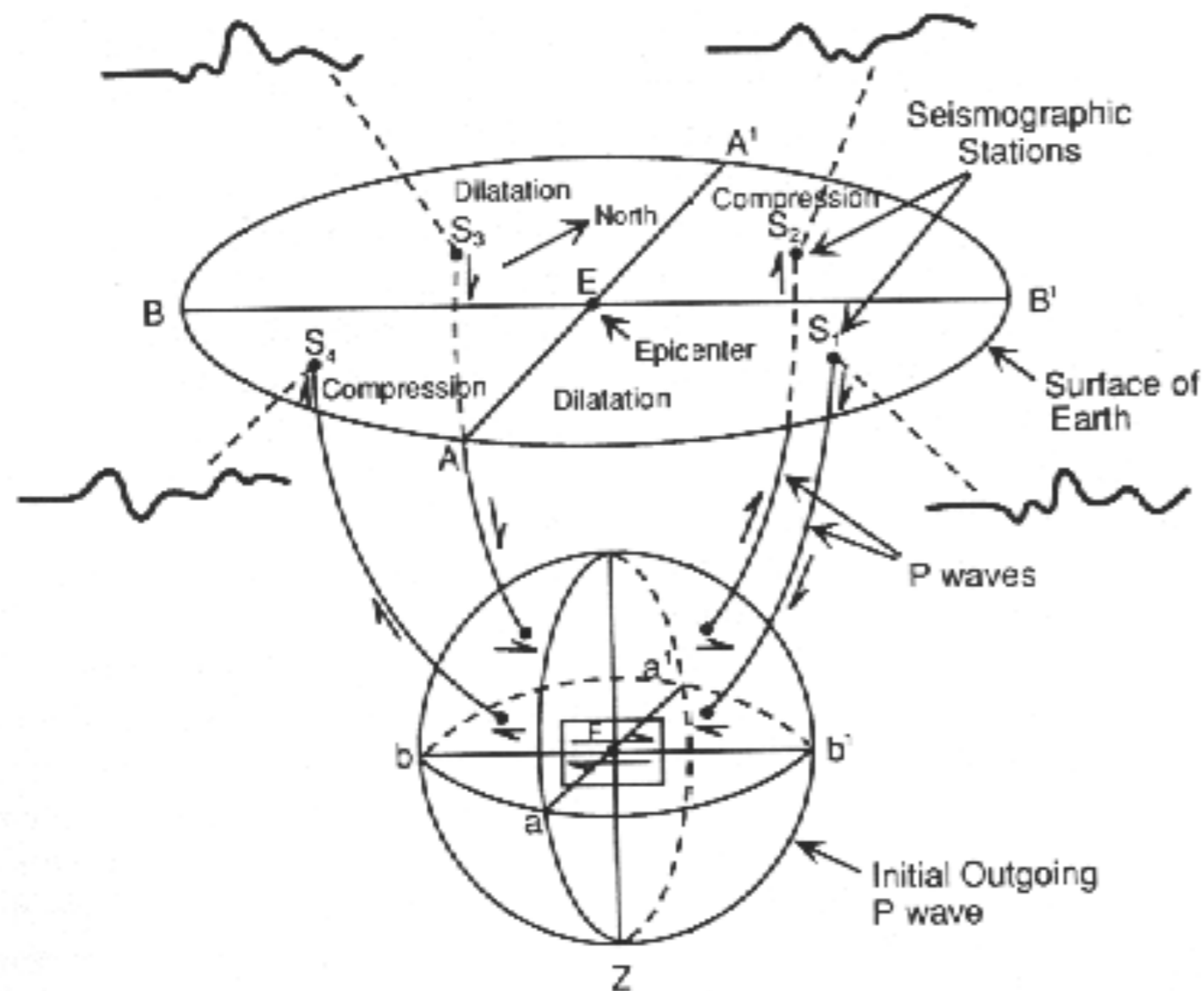


Radiation from shear dislocation

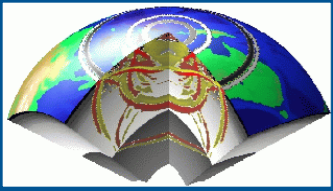


First motion of P waves at seismometers in various directions.

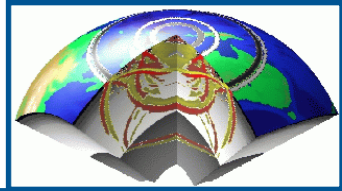
The polarities of the observed motion is used to determine the point source characteristics.



Beachballs always have two curved lines separating the quadrants, i.e. they show two planes. But there is only one fault plane and the other is called the auxiliary plane. Seismologists cannot tell which is which from seismograms alone, so we always show both of the possible solutions.

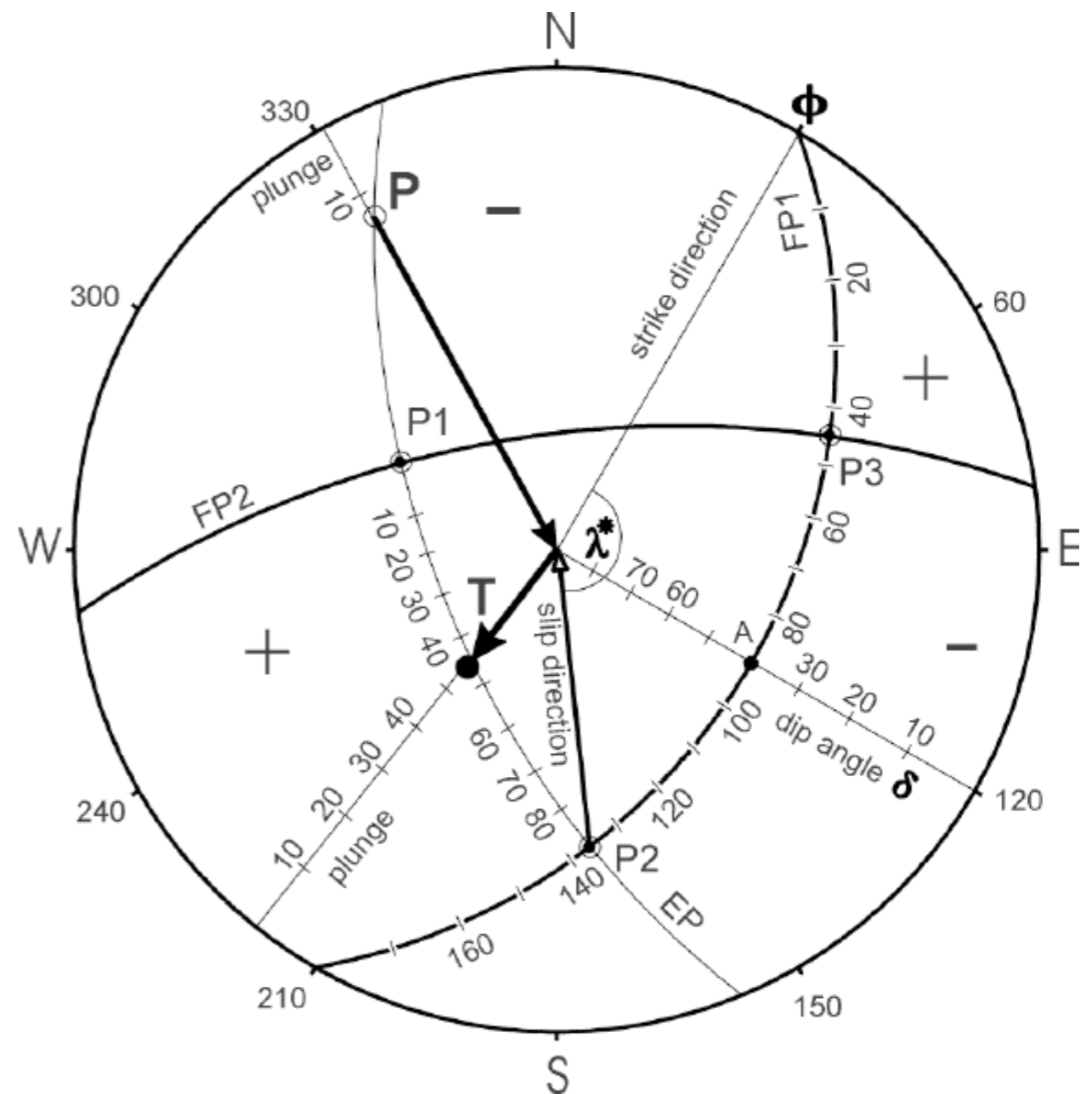


Manual determination of focal mechanism



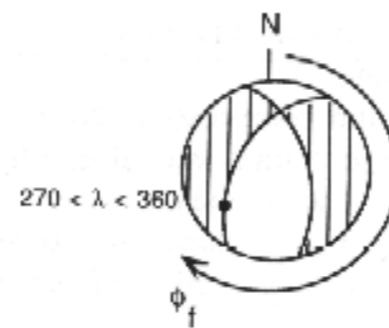
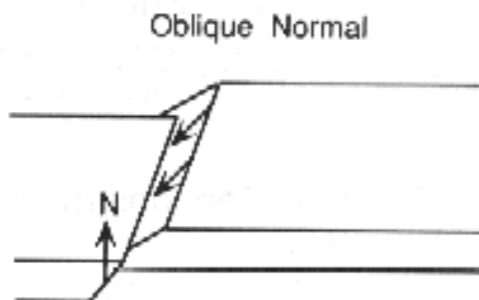
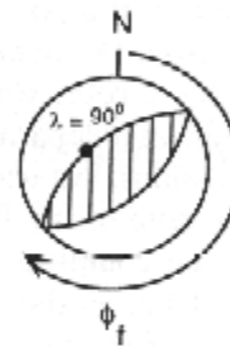
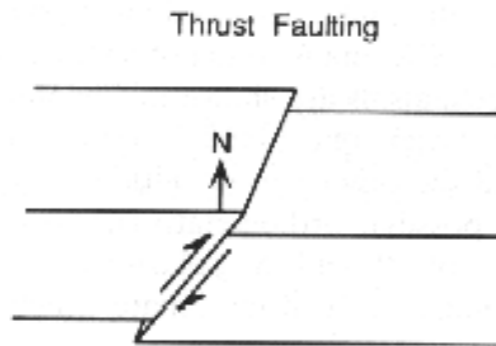
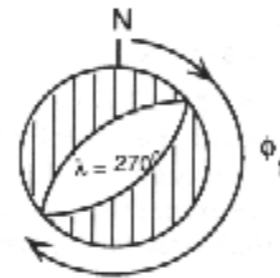
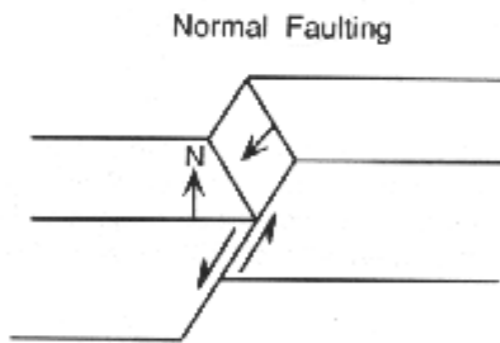
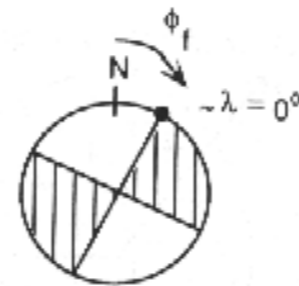
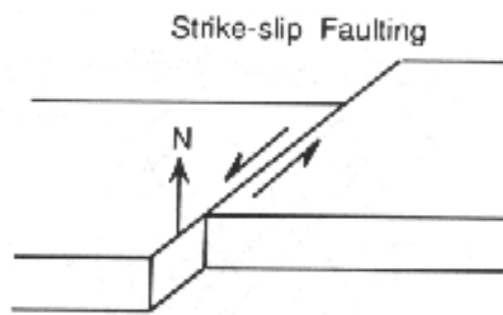
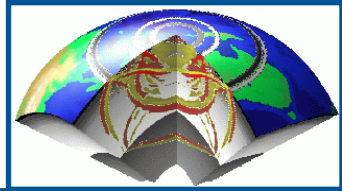
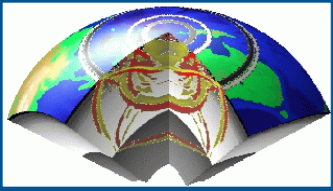
To obtain a fault plane solution basically three steps are required:

1. Calculating the positions of the penetration points of the seismic rays through the focal sphere which are defined by the ray azimuth and the take-off angle of the ray from the source.
2. Marking these penetration points through the upper or lower hemisphere in a horizontal (stereographic) projection sphere using different symbols for compressional and dilatational first arrivals.
3. Partitioning the projection of the lower focal sphere by two perpendicular great circles which separate all (or at least most) of the + and - arrivals in different quadrants.

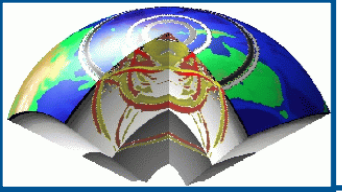


Note: $\lambda^* = 180^\circ - \lambda$ when the center of the net lies in the tension (+) quadrant (i.e., event with thrust component) or $\lambda^* = -\lambda$ when the center of the net lies in the pressure quadrant (i.e., event with normal faulting component). P1, P2 and P3 are the poles (i.e., 90° off) of FP1, FP2 and EP, respectively. P and T are the penetration points (poles) of the pressure and tension axes, respectively, through the focal sphere. + and - signs mark the quadrants with compressional and dilatational P-wave first motions.

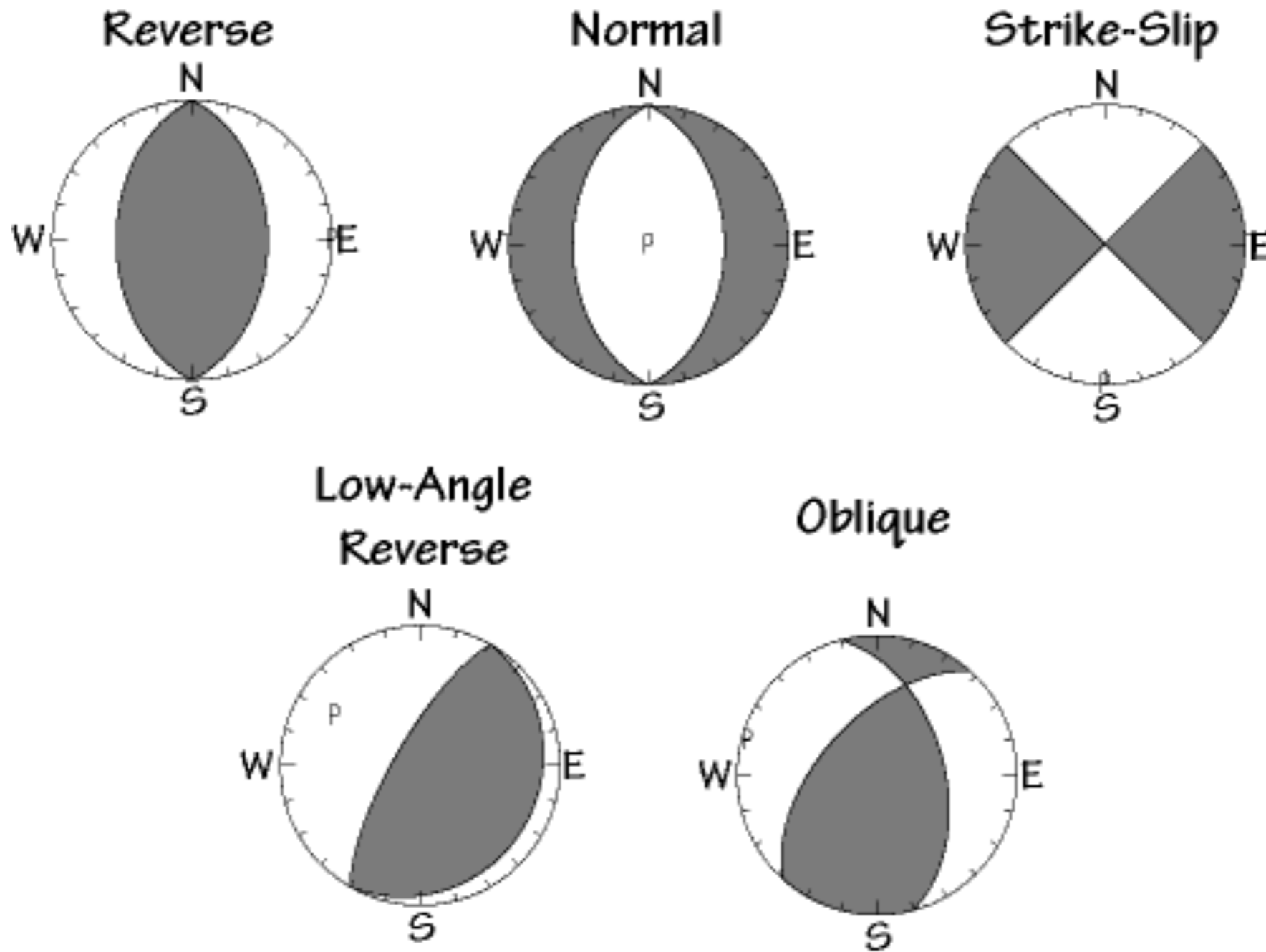
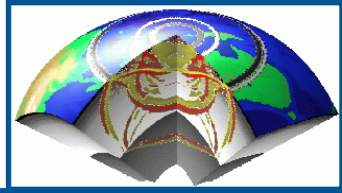
Fault types and focal mechanisms

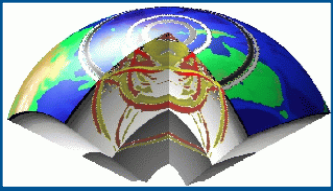


Basis fault types and their appearance in the focal mechanisms. Dark regions indicate compressional P-wave motion.



The Principal Mechanisms





FM & stress axes

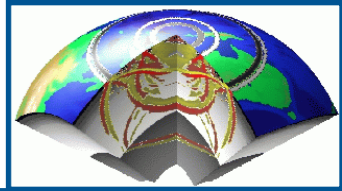
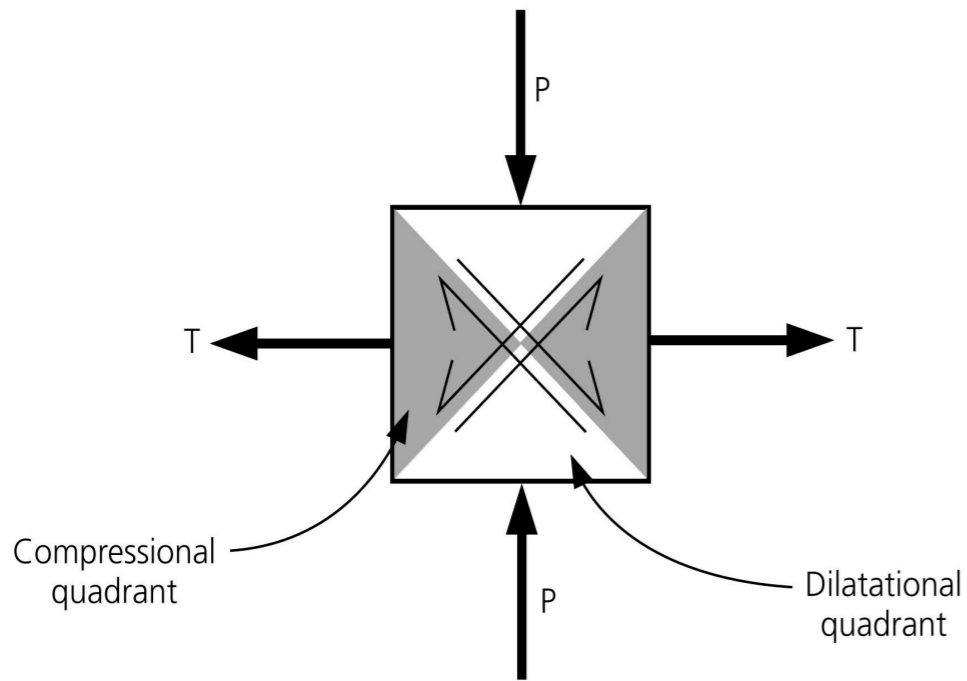
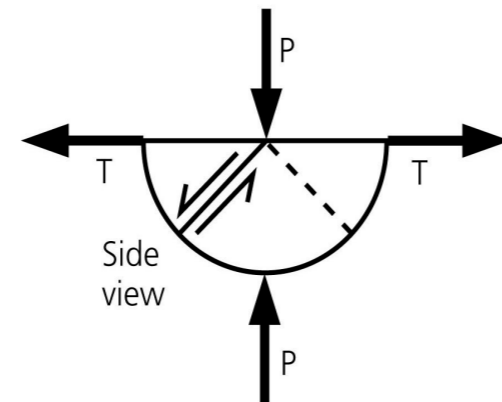
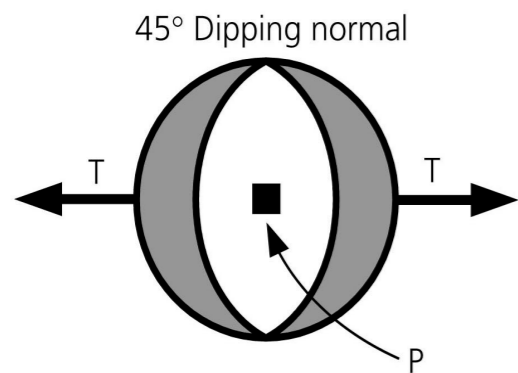
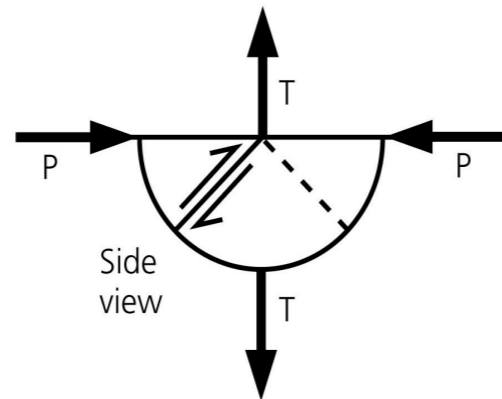
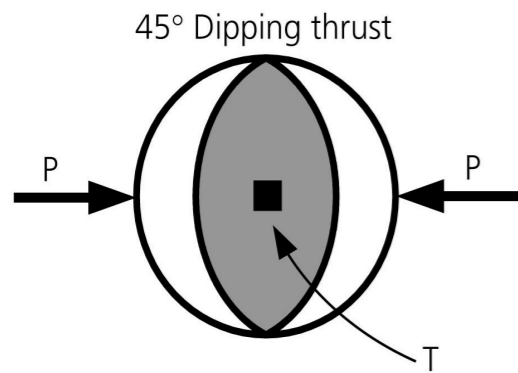


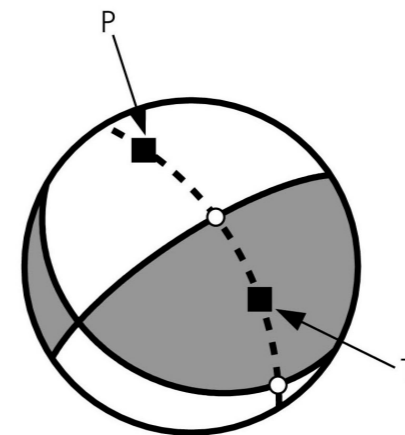
Figure 4.2-16: Relation between fault planes and stress axes.



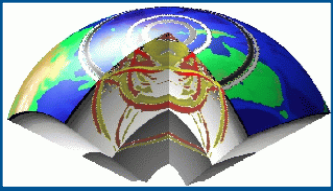
Faults



To obtain P and T axes:



On the meridian connecting the poles, the points half-way between the nodal planes are the **P** and **T** axes



Focal Mechanisms - Examples

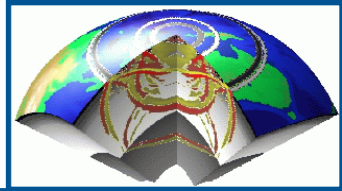
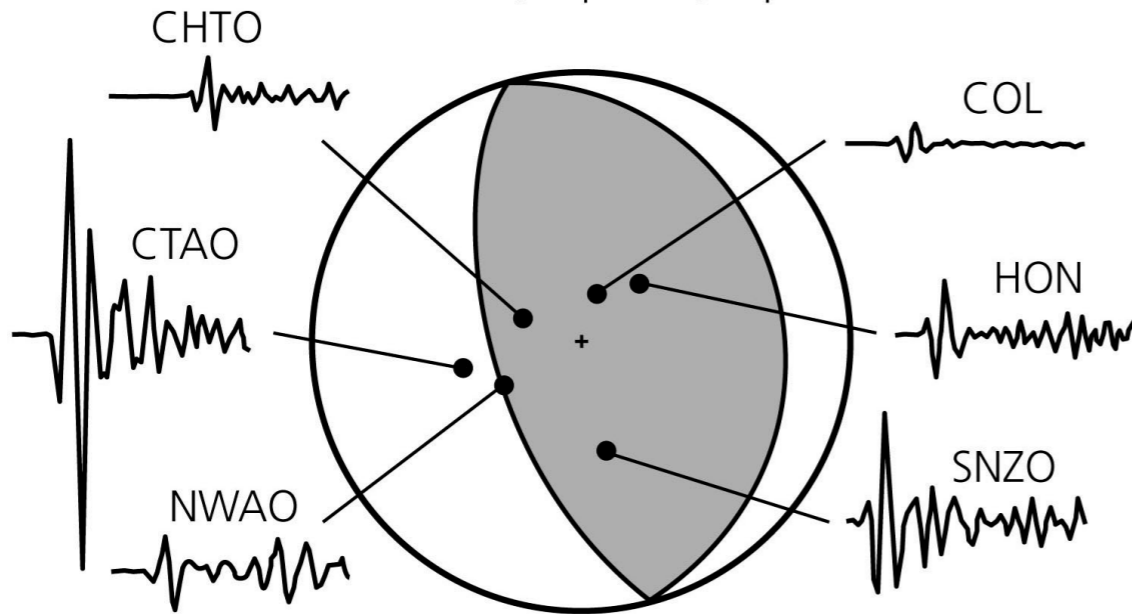


Figure 4.2-17: Examples of focal mechanisms and first motions.

Thrust faulting, Vanuatu Islands, July 3, 1985

Location: 17.2°S, 167.8°E. Depth: 30 km

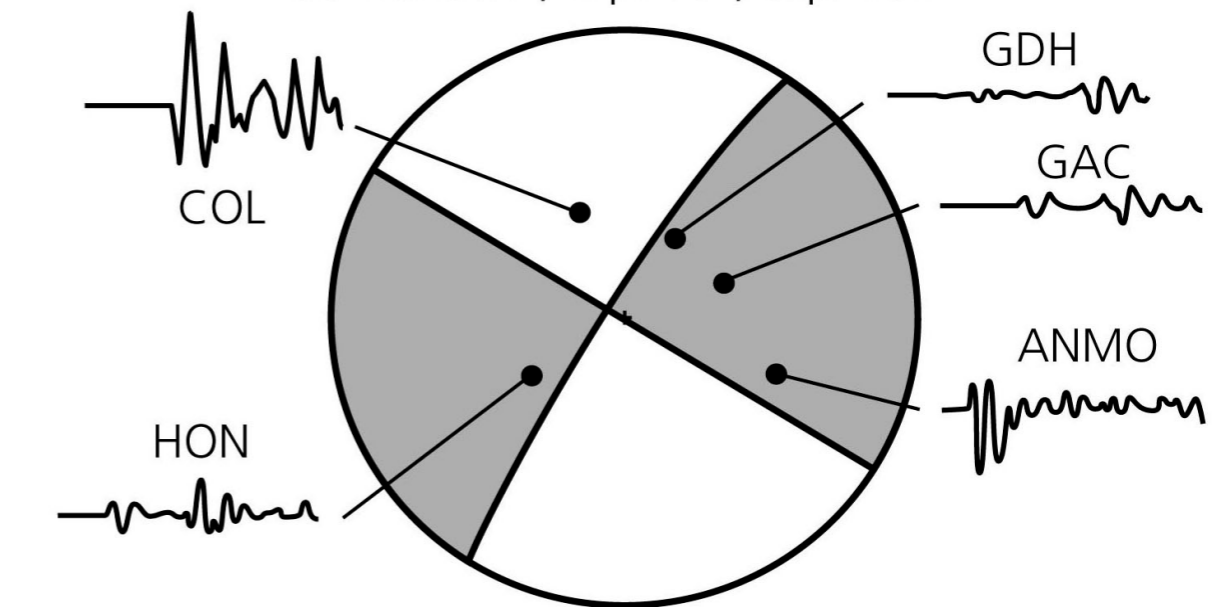
Strike: 352°, Dip: 26°, Slip: 97°



Strike-slip faulting, west of Oregon, March 13, 1985

Location: 43.5°N, 127.6°W. Depth: 10 km

Strike: 302°, Dip: 90°, Slip: 186°

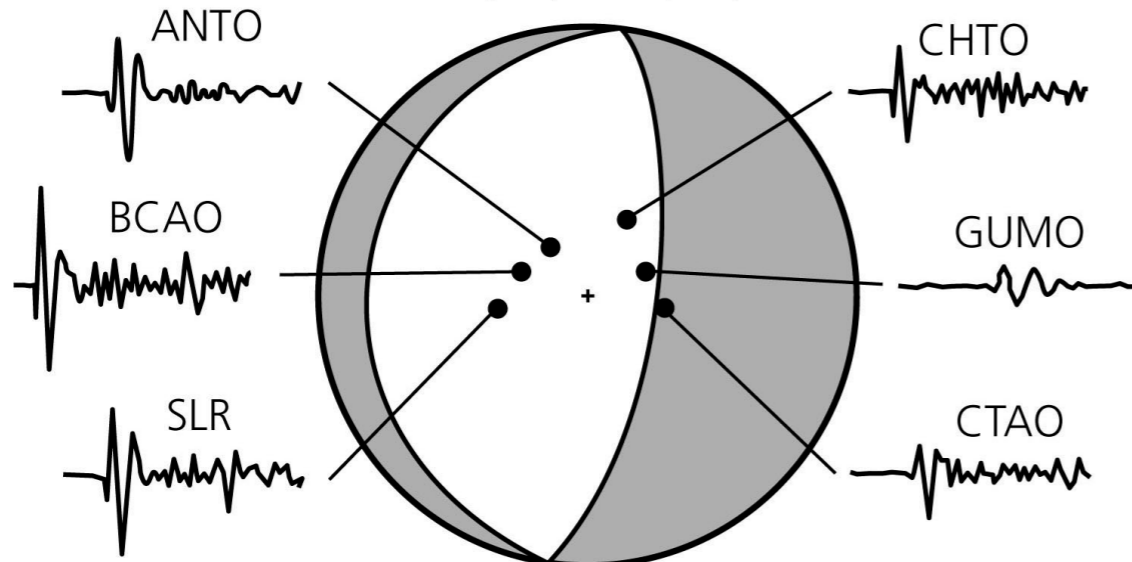


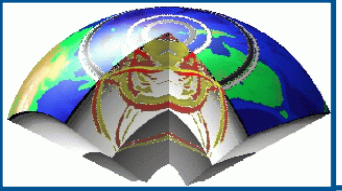
0 120 240
(s)

Normal faulting, mid-Indian rise, May 16, 1985

Location: 29.1°S, 77.7°E. Depth: 10 km

Strike: 8°, Dip: 70°, Slip: 270°





Double couple RP & surface waves

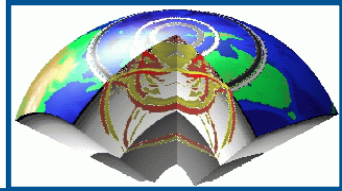
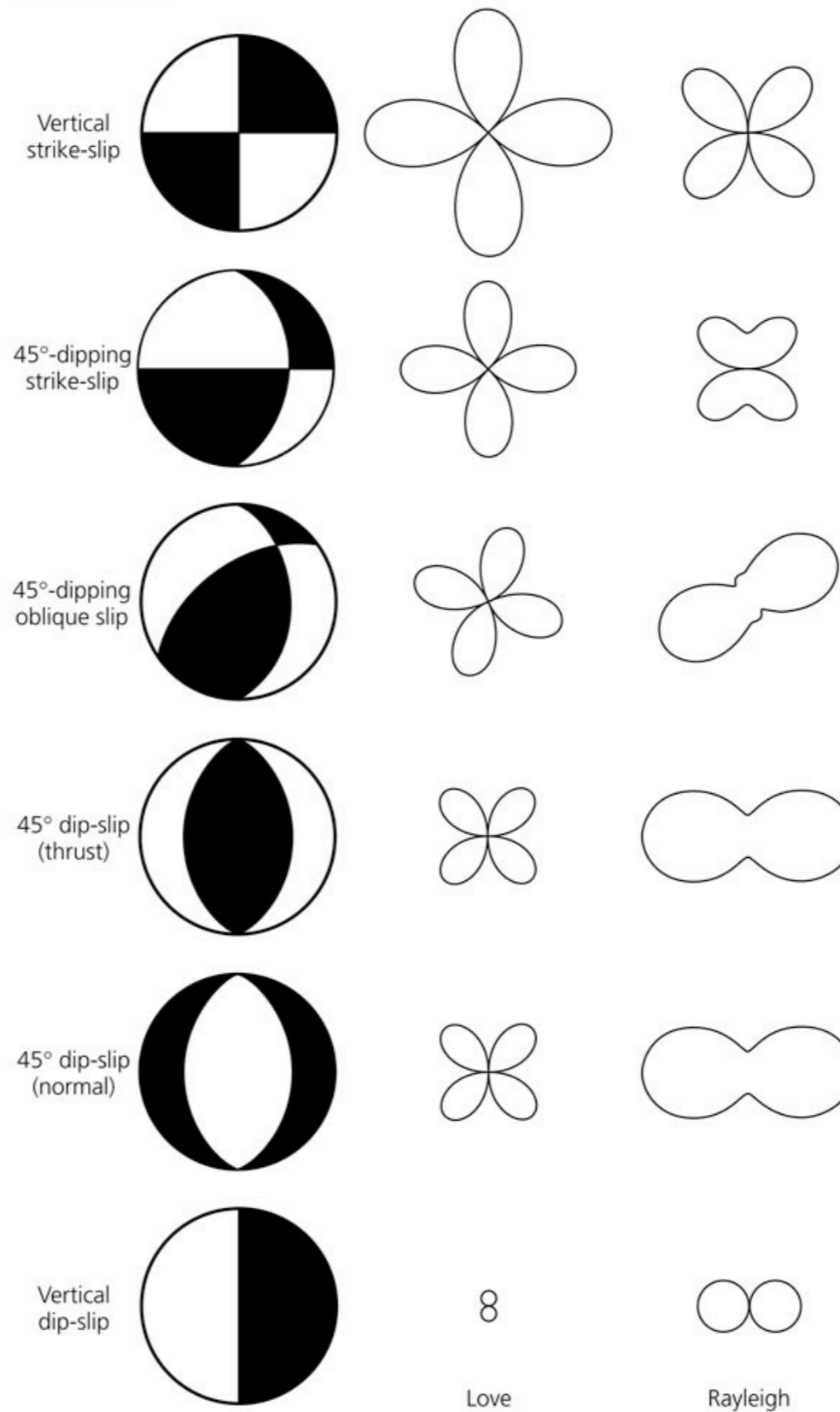
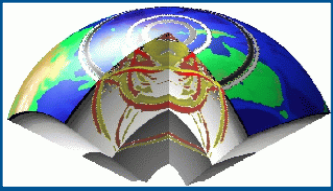


Figure 4.3-12: Surface wave amplitude radiation patterns for several focal mechanisms.





FM & Moment tensor

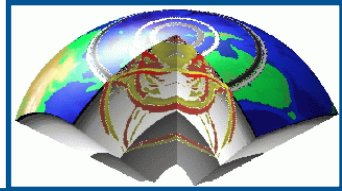
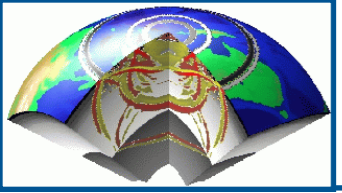
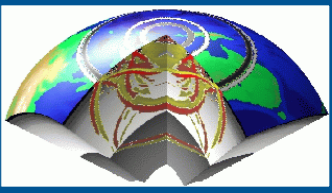


Figure 4.4-6: Selected moment tensors and their associated focal mechanisms.

Moment tensor	Beachball	Moment tensor	Beachball
$\frac{1}{\sqrt{3}} \begin{pmatrix} 1 & 0 & 0 \\ 0 & 1 & 0 \\ 0 & 0 & 1 \end{pmatrix}$		$-\frac{1}{\sqrt{3}} \begin{pmatrix} 1 & 0 & 0 \\ 0 & 1 & 0 \\ 0 & 0 & 1 \end{pmatrix}$	
$-\frac{1}{\sqrt{2}} \begin{pmatrix} 0 & 1 & 0 \\ 1 & 0 & 0 \\ 0 & 0 & 0 \end{pmatrix}$		$\frac{1}{\sqrt{2}} \begin{pmatrix} 1 & 0 & 0 \\ 0 & -1 & 0 \\ 0 & 0 & 0 \end{pmatrix}$	
$\frac{1}{\sqrt{2}} \begin{pmatrix} 0 & 0 & -1 \\ 0 & 0 & 0 \\ -1 & 0 & 0 \end{pmatrix}$		$\frac{1}{\sqrt{2}} \begin{pmatrix} 0 & 0 & 0 \\ 0 & 0 & -1 \\ 0 & -1 & 0 \end{pmatrix}$	
$\frac{1}{\sqrt{2}} \begin{pmatrix} -1 & 0 & 0 \\ 0 & 0 & 0 \\ 0 & 0 & 1 \end{pmatrix}$		$\frac{1}{\sqrt{2}} \begin{pmatrix} 0 & 0 & 0 \\ 0 & -1 & 0 \\ 0 & 0 & 1 \end{pmatrix}$	
$\frac{1}{\sqrt{6}} \begin{pmatrix} 1 & 0 & 0 \\ 0 & -2 & 0 \\ 0 & 0 & 1 \end{pmatrix}$		$\frac{1}{\sqrt{6}} \begin{pmatrix} -2 & 0 & 0 \\ 0 & 1 & 0 \\ 0 & 0 & 1 \end{pmatrix}$	
$\frac{1}{\sqrt{6}} \begin{pmatrix} 1 & 0 & 0 \\ 0 & 1 & 0 \\ 0 & 0 & -2 \end{pmatrix}$		$-\frac{1}{\sqrt{6}} \begin{pmatrix} 1 & 0 & 0 \\ 0 & 1 & 0 \\ 0 & 0 & -2 \end{pmatrix}$	



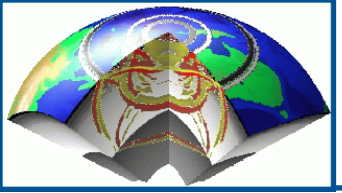
Faults and Plates



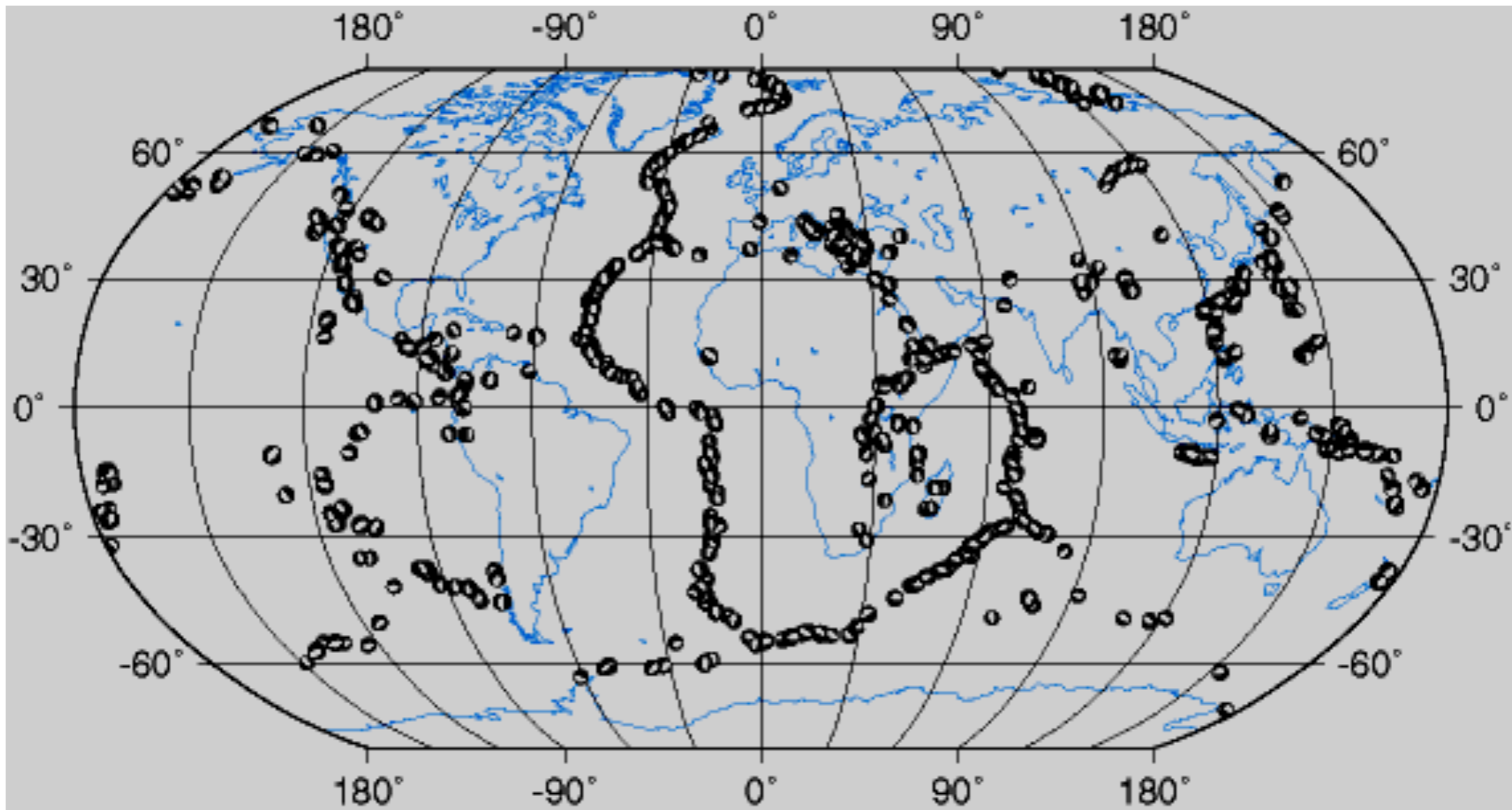
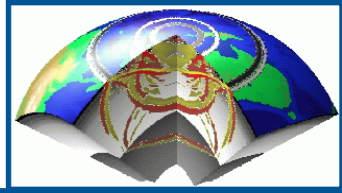
The style of faulting tells us something about the forces acting in a particular part of Earth.

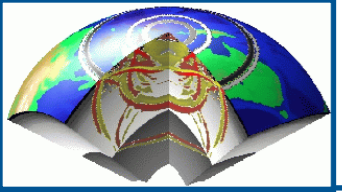
Along plate boundaries, faulting reflects the motion of plates.

- Divergent Boundary = Normal Faulting
- Convergent Boundary = Reverse Faulting
- Transform Boundary = Strike-Slip Faulting

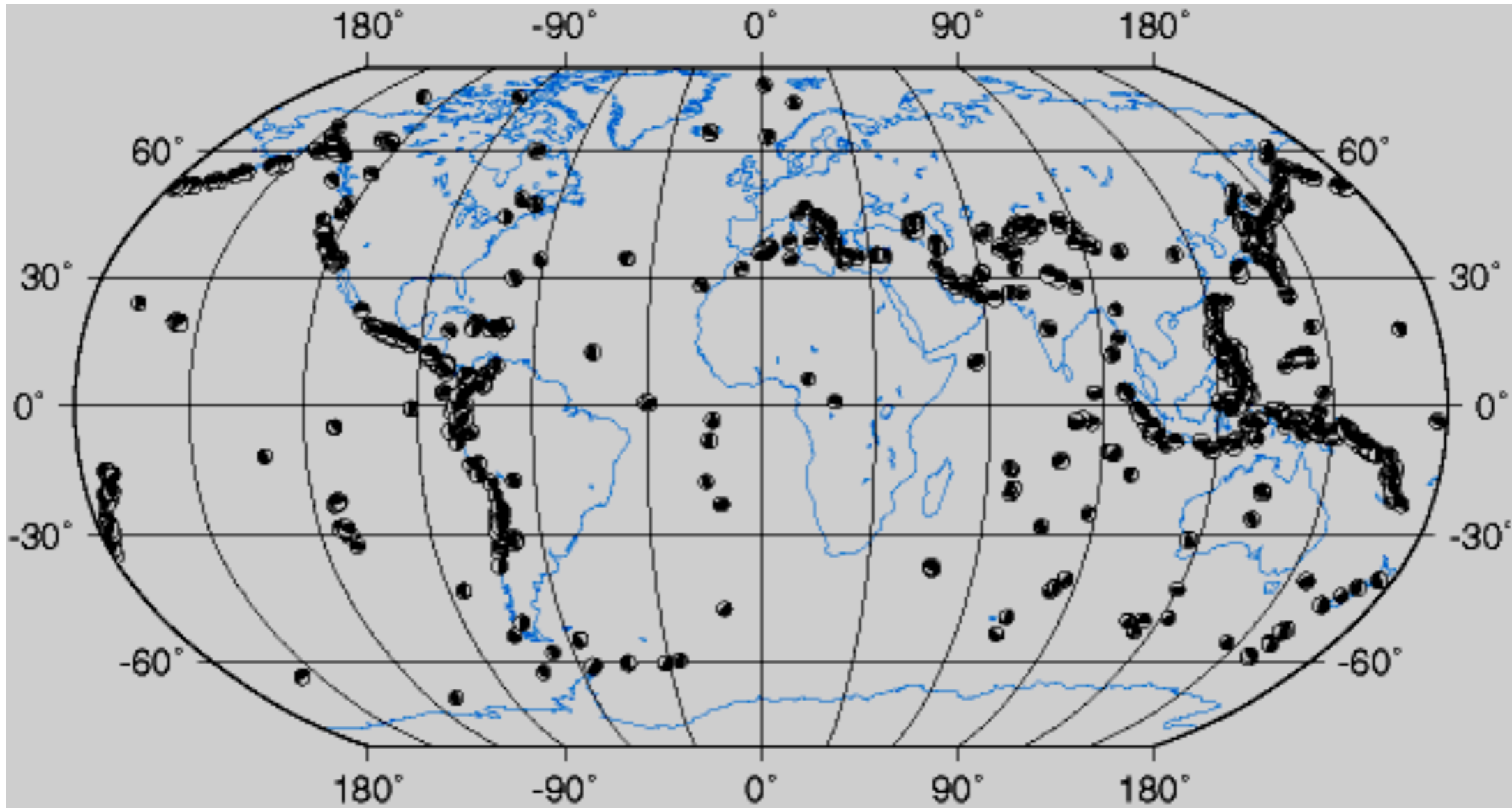
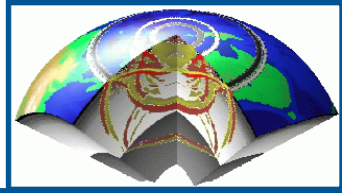


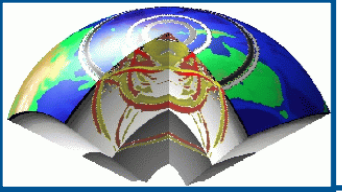
Where are the Normal Faults?



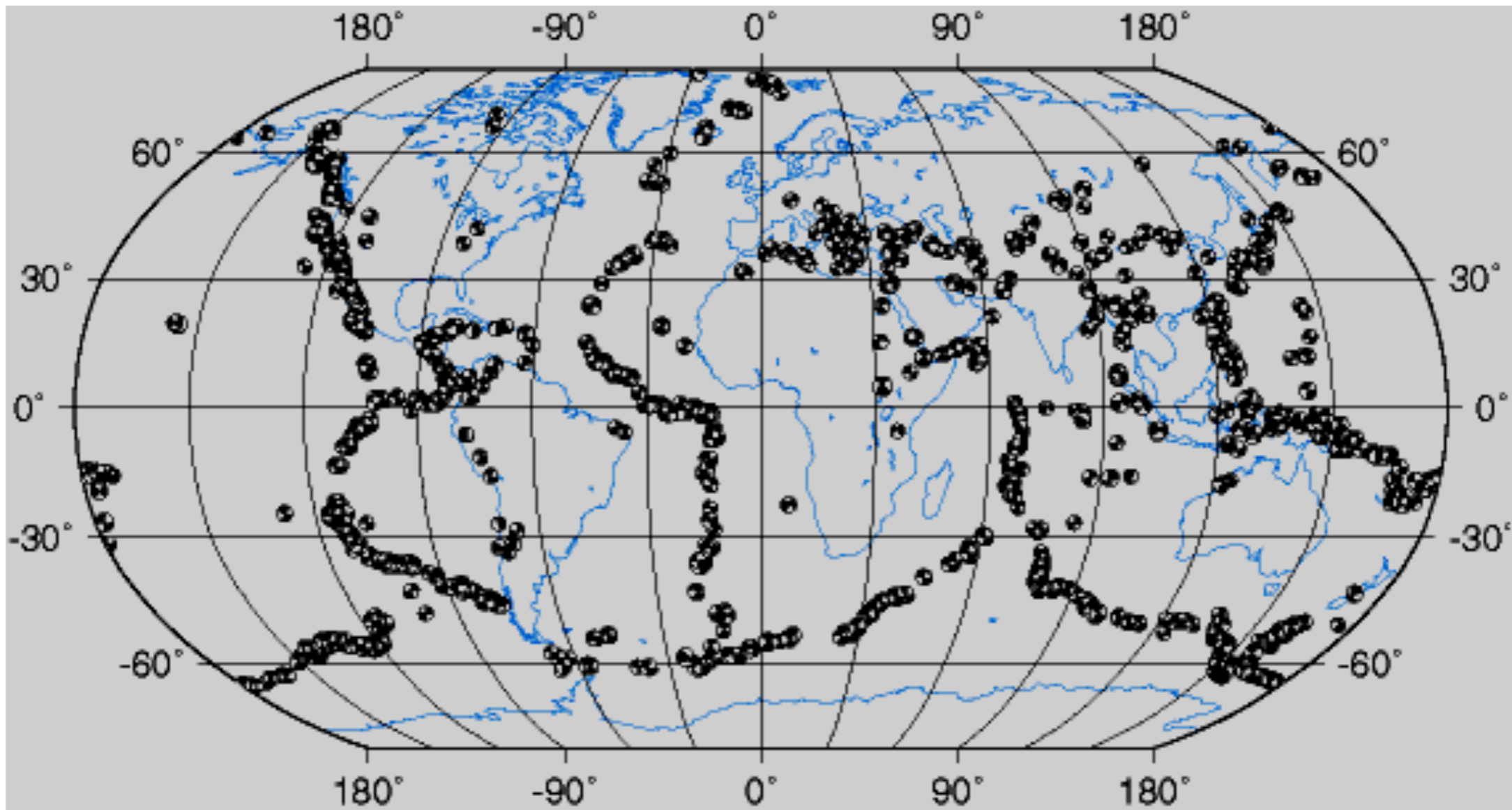
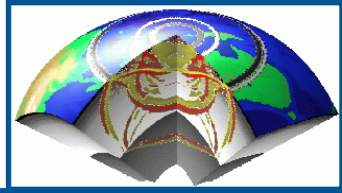


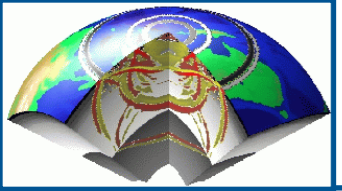
Where are the Reverse Faults?



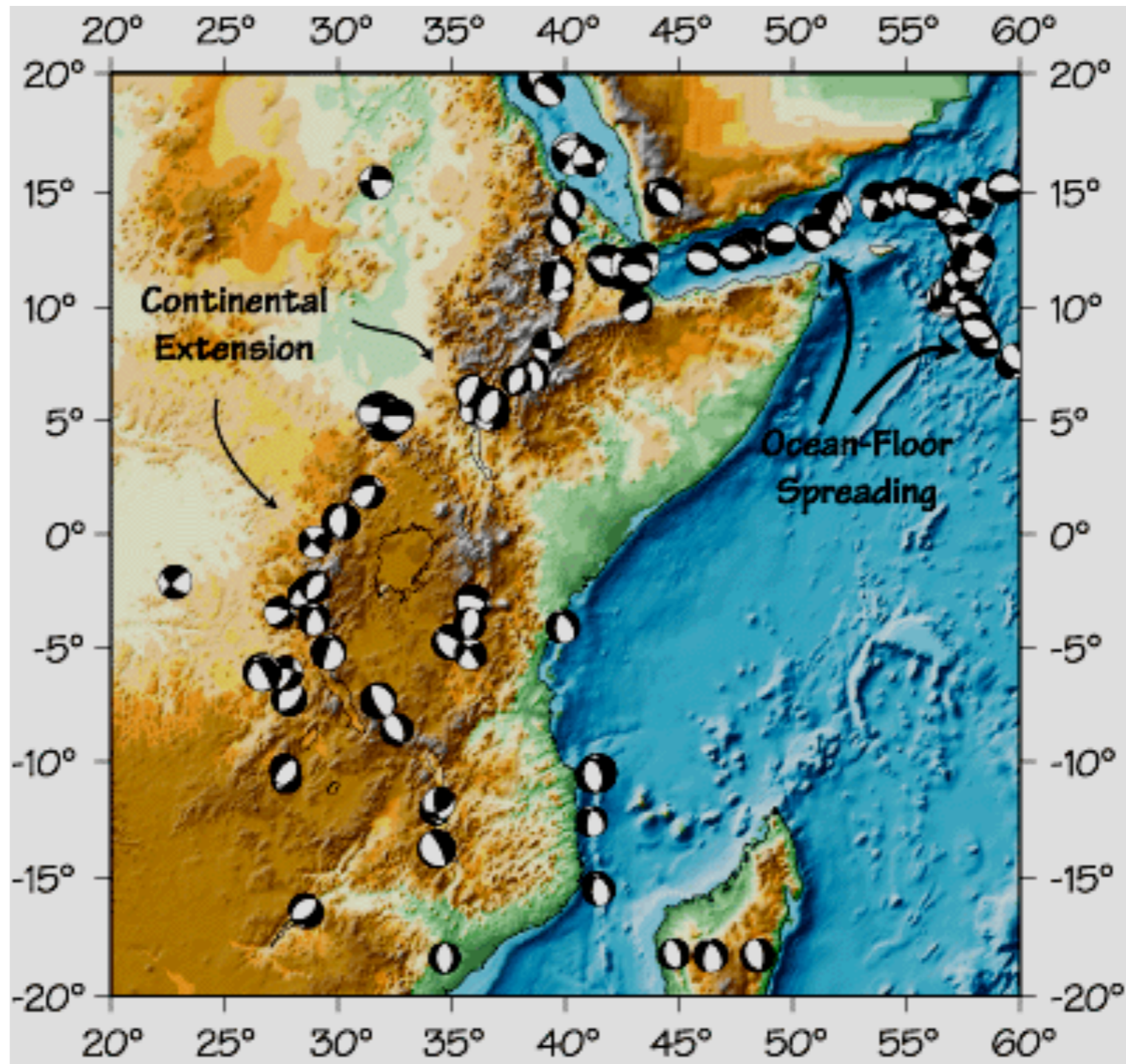
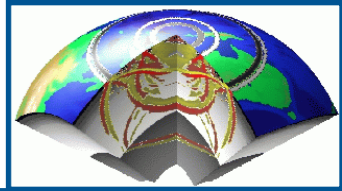


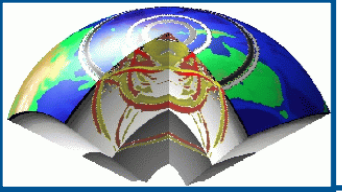
Where are the Transform Faults?



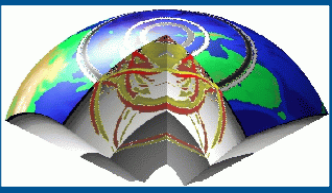


Example: East Africa

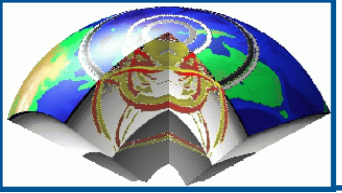




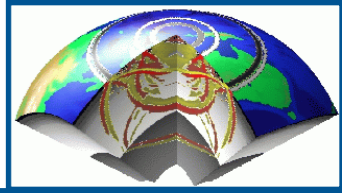
Faulting



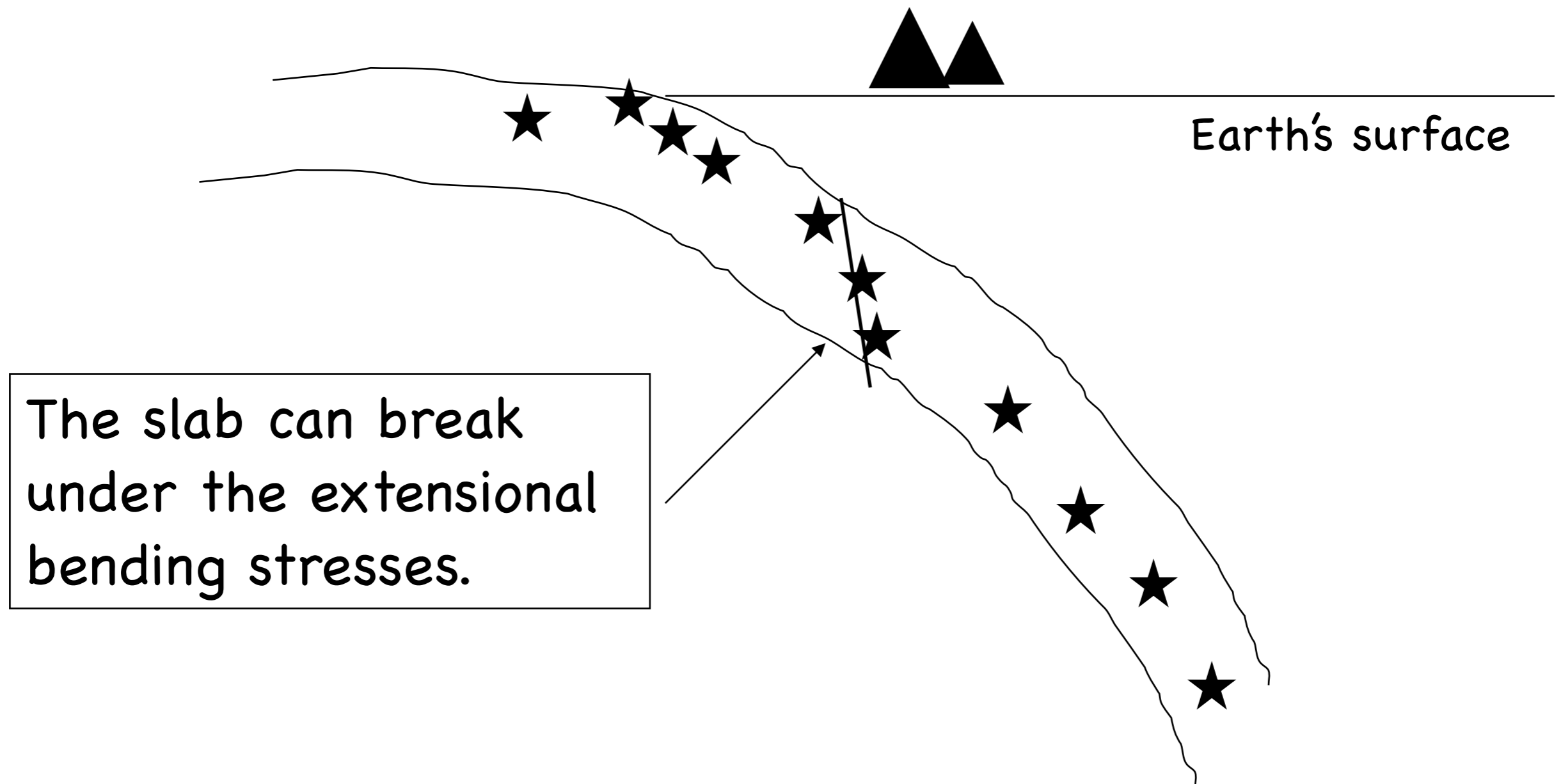
- So far we have talked about the faulting of shallow earthquakes, which are well explained by plate tectonics.
- What about the faulting style of deep earthquakes ?
- Do similar principles hold true?

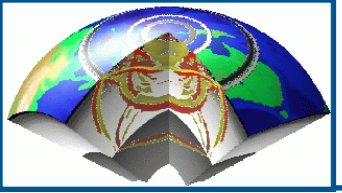


Faulting

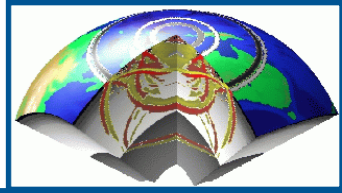


- We sometimes see “normal” faulting at depths of 100 km or so in subduction zones:





Faulting



- We sometimes see “reverse” faulting for the deepest earthquakes at about 600 km depth:

